ELSEVIER

PEPTIDES

Peptides 20 (1999) 695–712

Structure, distribution, and biological activity of novel members of the allatostatin family in the crayfish *Orconectes limosus*

Heinrich Dircksen[a,*], Petra Skiebe[b], Britta Abel[a], Hans Agricola[c], Klaus Buchner[d], J. Eric Muren[e], Dick R. Nässel[e]

[a]*Institute of Zoophysiology, University of Bonn, Bonn 53115, Germany*
[b]*Institute of Neurobiology, Freie Universität Berlin, Berlin 14195, Germany*
[c]*Institute of General Zoology and Animal Physiology, University of Jena, Jena 07743, Germany*
[d]*Institute of Biochemistry, Freie Universität Berlin, Berlin 14195, Germany*
[e]*Department of Zoology, Stockholm University, Stockholm 10691, Sweden*

Received 25 November 1998; accepted 8 February 1999

Abstract

In the central and peripheral nervous system of the crayfish, *Orconectes limosus*, neuropeptides immunoreactive to an antiserum against allatostatin I (= Dipstatin 7) of the cockroach *Diploptera punctata* have been detected by immunocytochemistry and a sensitive enzyme immunoassay. Abundant immunoreactivity occurs throughout the central nervous system in distinct interneurons and neurosecretory cells. The latter have terminals in well-known neurohemal organs, such as the sinus gland, the pericardial organs, and the perineural sheath of the ventral nerve cord. Nervous tissue extracts were separated by reverse-phase high-performance liquid chromatography and fractions were monitored in the enzyme immunoassay. Three of several immunopositive fractions have been purified and identified by mass spectroscopy and microsequencing as AGPYAFGL-NH_2, SAGPYAFGL-NH_2, and PRVYGFGL-NH_2. The first peptide is identical to carcinustatin 8 previously identified in the crab *Carcinus maenas*. The others are novel and are designated orcostatin I and orcostatin II, respectively. All three peptides exert dramatic inhibitory effects on contractions of the crayfish hindgut. Carcinustatin 8 also inhibits induced contractions of the cockroach hindgut. Furthermore, this peptide reduces the cycle frequency of the pyloric rhythms generated by the stomatogastric nervous system of two decapod species in vitro. These crayfish allatostatin-like peptides are the first native crustacean peptides with demonstrated inhibitory actions on hindgut muscles and the pyloric rhythm of the stomatogastric ganglion.

Keywords: Neuropeptide; Allatostatin; Hindgut; Stomatogastric ganglia; *Orconectes limosus*; *Leucophaea maderae*; *Cancer pagurus*; *Cherax destructor*

1. Introduction

A set of neuropeptides that inhibit juvenile hormone biosynthesis in the corpora allata was isolated from the cockroach *Diploptera punctata* [72]. These closely related peptides were thus designated allatostatins. Subsequently, a large number of related neuropeptides has been isolated from several other insect species of the orders *Orthoptera, Diptera, Lepidoptera,* and *Blattoidea* [12,18,20,22,71,72, 75,79,81,83]. Although these peptides are not inhibiting juvenile hormone synthesis in all the insect species of origin, they have been referred to the peptide family of allatostatins, because most of them share the common amidated C-terminus YXFGLamide. The analysis of precursor structures has revealed that up to 14 neuropeptides belonging to this class occur on the same precursor in the cockroaches *D. punctata* and *Periplaneta americana* and the locust *Schistocerca gregaria* [13,17,78,83]. Recently, in the two blowfly species *Calliphora vomitoria* and *Lucilia cuprina*, genes have been cloned that contain identical sequences of five allatostatin-like peptides, almost all of which have been identified before as so-called Leu-callatostatins from extracts of fly heads [22]. It is noteworthy that some callatostatins (Leu-Cast 2, 3, and 8) identified before from extracts of fly central nervous system (CNS) [21] can now be considered products of N-terminal trimming or cleavage during

* Corresponding author. Tel.: +49-228-732-472; fax: +49-228-732-496.
E-mail address: Dircksen@uni-bonn.de (H. Dircksen)

0196-9781/99/$ – see front matter
PII: S0196-9781(99)00052-2

processing of the peptides encoded on the precursor (e.g. from those designated II and V [22]). Apart from the functions as true allatostatic factors, which seem to be restricted only to a subgroup of peptides of this family and to certain insect species, the cockroach allatostatins and the blowfly callatostatins have been shown to exhibit inhibitory actions on parts of the insect gut. In homologous assays, by using the species from which the peptides were isolated, both the cockroach and the fly peptides display inhibitory actions on the hindgut with some restriction to the ileal part [22,38]. It is surprising, however, that when tested in a heterologous assay by using the cockroach *Leucophaea maderae*, a species in which only one allatostatin-like peptide is known [47], callatostatins exert inhibitory effects only on the foregut but not on the hindgut of this species [23]. Extensive immunocytochemical studies of allatostatin-like immunoreactive (ASTir) peptides in the CNS of insects have shown an abundant distribution of ASTir peptides not only in lateral protocerebral neurons innervating the corpora cardiaca and allata [70], but, furthermore, in interneurons of the entire CNS, in projection neurons extending to peripheral neurohemal and visceral organs including the hindgut, and even in gut endocrine cells of several insect species [2,12, 22,23,54,82].

Evidence for the existence of ASTir neurons in the central and peripheral nervous system of other invertebrate groups such as coelenterates, worms, mollusks, and crustaceans has further accumulated from immunocytochemical studies [1,10,55,60,63,64]. In crustaceans, for instance, the stomatogastric nervous system and the pericardial organs of the crab *Cancer borealis*, the lobster *Homarus americanus*, and the crayfish *Cherax destructor* and *Procambarus clarkii* [10,59,60] and the entire nervous systems of *Carcinus maenas* and the crayfish *Orconectes limosus* [1] have been shown to contain extensive neuronal systems reacting with antibodies against an insect allatostatin. Furthermore, physiological experiments have demonstrated profound inhibitory effects of some selected cockroach allatostatins on the rhythms generated by the stomatogastric nervous system (STNS) and on stomach muscles of *C. borealis* [34,60]. *D. punctata* allatostatins (Dip-AST) I to IV (= Dipstatins 7, 9, 8, and 5), but in particular Dip-AST III (= Dipstatin 8), inhibit the pyloric [60] and the gastric rhythms [61] generated by the stomatogastric ganglion (STG), in a dose-dependent manner. The same allatostatins were also able to reduce the amplitude of nerve-evoked contractions, excitatory junctional potentials, and excitatory junctional currents at both cholinergic and glutamatergic neuromuscular junctions [34]. Preliminary data from in vivo experiments with the crayfish *C. destructor* and *O. limosus* indicated that injections of Dip-AST III into the hemolymph reduce the number of spikes per cycle of some of the STG neurons and the frequency of the pyloric rhythm [7,30]. Recently, an unexpected multitude of up to 20 allatostatin-like peptides, termed carcinustatins, has been identified in extracts of thoracic ganglia of the green crab, *C. maenas* [19], the physiological actions of which are not yet known. However, the nature of native crayfish allatostatin-like peptides was up to the present date unknown.

In the present study, we describe the neuronal localization and quantitative distribution of ASTir material and the identification of the first three of several native allatostatin-like peptides in the CNS of the crayfish *O. limosus*. We provide physiological data on profound inhibitory effects of the peptides on the crayfish hindgut and, in the case of one of these peptides, on the pyloric rhythm generated by the neurons of the STG of a closely related crayfish and a crab species. In addition, the latter peptide was also tested in a heterologous insect hindgut preparation to see whether the observed close similarities in the primary structures of crayfish and insect allatostatin-like peptides might be indicative of functional similarities.

2. Materials and methods

2.1. Animals

American crayfish *O. limosus* from the river Havel in Berlin, Germany, were obtained from local fishermen and kept in large aquaria with running tap water at 12°C to 14°C and a light/dark cycle of 12:12 h. Specimens of the Australian crayfish *C. destructor* (60–90 g) were obtained from commercial dealers in Hamburg, Germany, and kept in running tap water at 14–16°C on a light/dark cycle of 12:12 h. Edible crabs, *Cancer pagurus* (100–800 g), were purchased from a marine biological station (Biologische Anstalt Helgoland, Helgoland, Germany). The crabs were maintained in aquaria with circulating aerated, artificial seawater at 14°C to 16°C. Cockroaches, *Leucophaea maderae*, were taken from a laboratory colony maintained at Stockholm University, Stockholm, Sweden. These cockroaches were raised at 25°C with a light/dark cycle of 16:8 h and were fed dog chow and water ad libitum. Adult crayfish, crabs, and cockroaches of both sexes were cold-anesthetized on ice for ≈30 min before dissection.

2.2. Immunochemical techniques

Immunocytochemistry was performed as described previously [15] on whole mount preparations and Vibratome sections of ganglia of crayfish *O. limosus* CNS after fixation in Stefanini's fixative [73] overnight at room temperature. Ganglia were dissected in an ice-chilled crayfish saline (mM: NaCl, 440; KCl, 11.3; $MgCl_2$, 26.3; $CaCl_2$, 13.3; Tris base, 11.0; maleic acid, 5.2; pH 7.4 to 7.5; modified from the study by Van Harreveld [77]) and pinned out in silicone-coated dishes before application of the fixative. After washing out the fixative with 0.1 M phosphate-buffered saline (PBS), pH 7.4, eyestalk and brains were embedded in an ovalbumin/gelatin mixture hardened overnight in 10% formalin in PBS. Vibratome sections (50 μm thick) were cut

on a Vibratome Model 1000 (Bachofer, Heidelberg, Germany) in chilled PBS and incubated free-floating in 2% normal goat serum in 0.1 M Tris-HCl-buffered saline, pH 7.4, containing 0.5% Triton X-100 and 150 mM NaCl (TBTX-0.5) for 1 h. The latter incubation as well as all the following were performed at room temperature. Overnight incubations in primary anti-Dip-AST I serum (code K1 [82]) diluted 1:10 000 to 1:20 000 in TBTX-0.5 were followed by incubation steps in goat anti-rabbit link antiserum (Nordic Labs, Tilburg, The Netherlands) diluted 1:50 in TBTX-0.5 for 1 h and finally in peroxidase–antiperoxidase complexes (Dakopatts, Hamburg, Germany) diluted 1:300 in TBTX-0.5 for 1 h. Washes for 3 × 10 min between and after the steps were done in the same 0.1 M Tris-HCl-buffered saline but containing 0.1% Triton X-100. The peroxidase reaction was performed in 0.01% H_2O_2 and 10 mg of diaminobenzidine tetrahydrochloride (Sigma, Deisenhofen, Germany) in 0.1 M PBS, pH 7.4, for 30 to 45 min under visual control. Immunostaining of whole mount preparations of ventral nerve cord ganglia, STGs, and neurohemal pericardial organs was performed exactly as described elsewhere [16], by using the peroxidase–antiperoxidase technique for detection and two primary anti-Dip-AST I sera (codes K1 and K8 [82]) used at dilutions of 1:5 000 to 1:8 000. Both antisera gave the same staining patterns. For morphological nomenclature, especially of brain structures, we largely follow a terminology described previously for several infraorders of decapod crustaceans including crayfish [56].

A sensitive competitive enzyme immunoassay (EIA) for Dip-AST I, similar to those described previously for other small peptides [37,54], has been developed: Microtiter plates (Maxisorp F16 NUNC, Wiesbaden, Germany) were coated overnight with 100 μl/well of a conjugate of Dip-AST I coupled covalently to human serum albumin (Sigma) via 1-ethyl-3′-(3-dimethylaminopropyl)carbodiimide (Sigma) at a ratio of 50:1:560 parts of Dip-AST I/human serum albumin/1-ethyl-3′-(3-dimethylaminopropyl)carbodiimide [62] and diluted with 0.1 M phosphate buffer, pH 8.0, the final concentration being adjusted to 0.2 μg/ml of the human serum albumin carrier. After washing three times in 0.1 M phosphate buffer, pH 8.0, plates were blocked with 100 μl/well of 1% normal goat serum (Paesel, Frankfurt, Germany) in 0.1 M phosphate buffer, pH 8.0, for 2 h at room temperature or overnight at 4°C followed by chucking out the solution without further washes. Thereafter, samples and standards (50 μl/well) were applied at appropriate dilutions in 0.01 M PBS containing 8 g/l NaCl, 0.2 g/l KCl, and 0.1% Tween 20 (PBST) followed by 50 μl/well of the same anti-Dip-AST I antibodies as used for immunocytochemistry (code K1 mostly in use) both at a dilution of 1:4 000 in PBST were loaded onto the plates, mixed by briefly shaking, and incubated overnight at 4°C. After four washes in PBST, the detection of bound antibodies was accomplished by incubation for 1 h at room temperature of 100 μl/well of a sheep anti-rabbit peroxidase conjugate (Merck, Darmstadt, Germany) diluted 1:4000 in PBST. After another four washes in PBST, the enzyme reaction was performed for 30 to 45 min by using 0.006% H_2O_2 and 0.4 mg/ml 2-2′-azinobis-(3-ethylbenzthiazoline-6-sulfonic acid) (ABTS; Sigma) in sodium citrate buffer, pH 4.0. Absorbance was quantitatively evaluated at 405 nm in a plate reader (Titertek Multiscan Plus, Labsystems, Finland) connected to a personal computer (EIA program version 2.0, Flow Laboratories, Dunn, Asbach, Germany).

2.3. Extraction and prepurification of crayfish nervous tissues

To determine quantitatively the distribution of ASTir peptides in eyestalks, brains, and ventral nerve cord ganglia of *O. limosus*, tissues were carefully dissected in total under chilled crayfish saline subsequently cut between single ganglia complexes, as shown in Fig. 2. Each ganglion of three different specimens was extracted separately by a 30-s sonication in Eppendorf caps on ice (Branson sonifier, Branson, Danbury, CT, USA) in 500 μl of Bennett's acidic extraction medium consisting of 1% NaCl (wt/vol), 5% formic acid (vol/vol), 1% trifluoroacetic acid (TFA; vol/vol) in 1 M aqueous HCl [5], and centrifuged at 12 000 × *g* at 4°C in a Beckman microfuge (Beckman Instruments, Palo Alto, CA, USA). Supernatants were subsequently dried in a vacuum centrifuge (Speed Vac concentrator, Savant, Farmingdale, NY, USA). The remaining pellets were dissolved in 1 M NaOH for the determination of protein contents [65].

For the large-scale extraction and identification of ASTir peptides from initially two batches of CNS tissues of *O. limosus*, we modified methods described previously for the isolation of crab and cockroach myotropic peptides [9,48]. Extracts of a batch of 226 brains and 433 abdominal ganglia chains (5.23 g wet weight), and another batch of 252 ganglia chains of the thorax including the subesophageal and the five leg ganglia (7.61 g wet weight), were pooled at the end of the following procedure: Each batch of tissue was first homogenized in ≈20 ml of ice-cold Bennett's solution [5] in a hand-driven 50-ml Potter-Eveljem homogenizer with a Teflon pestle. The homogenate was then sonicated on ice for 4 × 30 s with a Vibra cell sonication system (Sonics and Materials, Danbury, CT, USA) and centrifuged at 10 500 × *g* for 20 min at 4°C in a Beckman J-21C centrifuge (JA20 rotor; Beckman Instruments). The resulting supernatant was stored on ice until being combined with the supernatant after reextraction of the pellet with the same method. The pooled supernatants were subjected to prepurification on Sep-Pak Vac 20cc C18 cartridges (Waters, Milford, MA, USA) equilibrated with 0.1% aqueous TFA after activation with 50 ml of 100% acetonitrile (MeCN) and 50 ml of 100% water before loading with extract samples. After washing off the unbound sample components on the cartridge with 10% aqueous MeCN containing 0.1% TFA (MeCN-TFA), peptides were eluted with 2 × 15 ml 40% aqueous MeCN-TFA.

2.4. Chromatography, mass spectrometry, microsequencing, and synthesis

Separation of peptides from crayfish *O. limosus* was performed by a modification of an established method [48] by reversed-phase high-performance liquid chromatography (HPLC) on a first Waters HPLC system with U6K injector, a Model 600E controller, and a Model 486 ultraviolet detector (set at 210 nm). Computerized data acquisition and processing with the aid of a Millennium 2010 chromatography manager was performed in the following four HPLC steps with four different column systems. If necessary, an additional purification step was performed on a second Waters HPLC system consisting of two Model 510 pumps, a Model 680 solvent programmer, a U6K injector, a Model 481 LC spectrophotometer (all Waters), and a chart recorder with integrator functions (Waters 740 Data Module). (1) For the first purification step, the Sep-Pak eluates were diluted to a final concentration of 10% MeCN-TFA. The final volume of ≈550 ml was divided in two batches of 225 ml and pumped in two separate runs directly onto a Delta-Pak RCM C18 cartridge (25 × 100 mm, 30 nm, 15 μm; Waters) within ≈30 min. After 1 min of initial conditions, a linear gradient was applied from 10% to 40% MeCN-TFA for 110 min (0.27% MeCN/min) followed by an isocratic mode in the same solvent for 7 min and a final 10-min gradient to 80% MeCN-TFA at a flow rate of 7.5 ml/min. Fractions were collected automatically every minute for 120 min and analyzed by the Dip-AST I EIA by taking out 150-μl subfractions from the 7.5 ml in each tube followed by drying in the Speed Vac concentrator, redissolving in 250 μl of EIA buffer, and assaying duplicates or triplicates of 50 μl of the latter, thus, finally an amount of 0.4% of each fraction per well. The remainders were saved frozen for a repetition of the EIA if necessary. Subsequently, immunopositive fractions were dried completely. (2) The pooled samples from two runs were taken up into 1 ml of 10% MeCN-TFA and subjected to the second HPLC step on a Vydac Diphenyl column (219TP54, 4.6 × 250 mm, 30 nm, 5 μm; Vydac, Hesperia, CA, USA). After 2 min under initial conditions, a linear gradient from 18% to 30% MeCN-TFA in 76 min (0.16% MeCN/min) was applied, which was followed by two short gradients of 1 min each to 40% and finally to 80% MeCN-TFA at a flow rate of 1 ml/min. Aliquots of 1% each of fractions collected automatically from 15 to 44 min were tested by EIA and immunopositive fractions were dried. (3) The third step, HPLC on a Supelcosil C8 column (LC-8-DB, 4.6 × 150 mm, 10 nm, 3 μm; Supelco, Bellefonte, PA, USA), made use, after 1 min under initial conditions, of a linear gradient from 10% to 30% MeCN-TFA in 60 min, followed by another short linear gradient to 40% MeCN-TFA in 5 min, an isocratic mode for 3 min, and finally, a linear gradient to 80% MeCN-TFA in 5 min at a flow rate of 1 ml/min. Aliquots of 1% of the peak fractions collected manually were tested by EIA and dried. (4) The fourth HPLC step, to purify the ASTir fractions eluted from the previous column, was performed on a Partisil C18 column (ODS3, 4.6 × 250 mm, 5 μm; Fisons Scientific Equipment, Leicestershire, UK) by using, after 2 min under initial conditions, a gradient from 15% to 35% MeCN-TFA in 40 min at a flow rate of 1 ml/min followed by the same final modes as described for the previous step. In another run performed on the same column, the gradient conditions were changed to an elution from 18% to 38% MeCN-TFA in 40 min. Aliquots of 1% of the manually collected fractions were tested by EIA. (5) The fifth HPLC step, performed on a Bakerbond C18 column (wide pore, 4.6 × 250 mm, 5 μm, Mallinckrodt Baker, Griesheim, Germany), involved, after 2 min under initial conditions, a gradient from 18% to 36% MeCN-TFA in 40 min, or to 33% MeCN-TFA in 50 min, at a flow rate of 1 ml/min. Aliquots of 1% of the manually collected fractions were tested by EIA.

Purified peptides were analyzed for molecular mass by matrix-assisted laser desorption/ionization mass spectrometry (MALDI-MS), by using either a Kompact MALDI II system (Kratos, Manchester, UK) at the Department of Medical and Physiological Chemistry, Uppsala University, Uppsala, Sweden, or a MALDI–time-of-flight (MALDI-TOF) system (Bruker, Bremen, Germany) at the Freie Universität Berlin, Berlin, Germany. Peptide samples (≈2 pmol of ASTir in the EIA) run on the MALDI-MS were reconstituted in 5 μl of 10% MeCN-TFA and applied at 0.5 μl together with an equal amount of α-cyano-4-hydroxycinnamic acid as a matrix. The spectra were externally calibrated. Peptide samples on the MALDI-TOF systems were reconstituted in 33% MeCN-TFA and applied with α-cyano-4-hydroxycinnamic acid (saturated in the same solution) as a matrix. Sample spectra were obtained in linear and/or reflectron mode at normal voltage. In addition, when only small quantities were available, peptides were subjected to post-source-decay analysis of their fragments [66] with emphasis on N-terminal b-ions detected at lower voltage in the reflectron mode [35].

Subsequently, Edman sequencing by the identification of phenylthiohydantoin-derivatized amino acids was performed on an Applied Biosystems Model 477A gas-phase protein sequencer equipped with a Model 120A analyzer (at Uppsala University) or on an Applied Biosystems Model 473A gas-phase protein sequencer (at Freie Universität, Berlin, Germany).

The peptides were synthesized on an Applied Biosystems Model 433A synthesizer by applying standard chemistry for 9-fluorenylmethyloxycarbonyl (Fmoc)-derivatized amino acids [3] at the Institute of Biochemistry, Charité Hospital, Humboldt University, Berlin, Germany. The purity of the synthetic peptide was checked on the second HPLC system. Solvents for a linear gradient elution were 0.11% TFA in H_2O and 60% MeCN-TFA. For details concerning columns and chromatographic conditions, see legends to Figs. 3 and 4. Synthetic peptides were quantified by amino acid analysis on reversed-phase HPLC according to

either orthophthaldialdehyde [84] or Fmoc-chloroformate [24] precolumn derivatization methods.

2.5. Bioassays

Established procedures for bioassaying of peptides were applied in a homologous bioassay of the heart and the hindgut of crayfish *O. limosus* [69] and in a heterologous bioassay of the hindgut of an insect, the cockroach *L. maderae* [32,48].

In brief, semiisolated crayfish hearts attached to the dorsal cephalothorax or the posterior half of the crayfish hindgut attached to a small piece of sternal and tergal cuticle surrounding the intact anus but dissected from the terminal ganglion connections were fixed within a cylindrical perfusion chamber (1.2 ml) and tied to a force transducer (FT 03, Grass Instruments, Quincy, MA, USA). Contraction frequencies and amplitudes were amplified with a preamplifier (7P122D, Grass Instruments) and recorded on a chart recorder (7S1225–79, Grass Instruments). The chamber was slowly and constantly perfused with the aid of a peristaltic pump with constantly aerated crayfish saline kept at 12°–14°C experimental temperature until the control or test samples were applied directly to the chamber. Only during sample application times the flow was stopped, which, however, had no influence on the contractile activity of the organs. Thereafter, the test samples were flushed out by using 20 ml of crayfish saline and perfusion started again for several minutes before the application of the next sample. Peptide samples were applied for 6 min by replacing 120 μl (10%) of the saline in the chamber by saline containing 10 times the desired final concentration of peptide. Analysis of contractions was performed by measuring their frequency and amplitude during 4 min before sample application and exactly between 1 and 5 min after sample application. For statistical analysis, a one-way analysis of variance test was applied at a 95% level of confidence.

For the cockroach hindgut assay, the dissected hindgut of *L. maderae* was attached under constantly aerated insect saline (mM: NaCl, 154; KCl, 2.7; $CaCl_2$, 1.8; glucose, 22; 4-(2-hydroxyethyl)-1-piperazineethanesulfonic acid (Hepes), 12; pH 6.75 [48]) by cotton thread loops with its posterior end to the bottom of a 5-ml glass chamber. The anterior end was attached to an isotonic tension transducer coupled to an amplifier (both from Kent Scientific Corp, Litchfield, CT, USA). Test samples were added to the saline in the chamber, and the tonus of the hindgut as well as the frequency and amplitude of spontaneous or stimulated contractions were recorded via a Servogor 120 pen recorder (Goerz, Neudorf, Austria). After incubation for at least 3 min, test samples were flushed out, and the hindgut was allowed to recover for at least 3 min before applying the next sample. Because no action was seen on spontaneous activity of the hindgut, synthetic CST-8 was applied for 3 min after a 3-min application of stimulation by proctolin or *Manduca sexta* allatotropin.

2.6. Electrophysiology

Further bioassay experiments were performed on the STNS of the crab *C. pagurus* and the crayfish *C destructor*. *C pagurus* was chosen because the STG has been shown to have the same identified cell types and network characteristics as the closely related species *C borealis* [29], which had previously been investigated for allatostatin effects [60]. The STNS output of the crayfish *O. limosus* proved to be extremely difficult to record over long periods especially after partial removal of the STG neural sheath, so the crayfish *C. destructor* was chosen for the electrophysiological experiments.

The STNS of both species is composed of four ganglia together with their connecting and motor nerves. The paired commissural ganglia (CoGs) lie between the brain and the subesophageal ganglion (SOG) (see also Fig. 9), which are interconnected by the circumesophageal connectives (*cocs*). The esophageal ganglion (OG) is located between and connected to both CoGs by the inferior esophageal nerves (*ions*). The STG is connected with the CoGs by the superior esophageal nerves (*sons*) and the stomatogastric nerve (*stn*). The main motor nerve leaving the STG is the dorsal ventricular nerve (*dvn*), which is a good monitor of the rhythms generated by the STG and from which all extracellular recordings were made.

Extracellular recordings were performed as described previously [60]. The dissected STNS from crab or crayfish was pinned down in a silicone polymer-lined (Sylgard 184, Dow Corning, Midland, MI, USA) Petri dish with a diameter of 5.5 cm and superfused with precooled 12° to 14°C *Cancer* saline (mM: NaCl, 440; $MgCl_2$, 26; $CaCl_2$, 13; KCl, 11; Trizma base, 10; maleic acid, 5; pH 7.4 to 7.5 [29]) or another crayfish saline (mM: NaCl, 205; $MgCl_2$, 2.6; $CaCl_2$, 13.6; KCl, 0.54; 4-(2-hydroxyethyl)-1-piperazineethanesulfonic acid, 7.6; pH 7.4 to 7.5; modified from the study by Van Harreveld [77]), respectively. The STGs were partially desheathed to facilitate diffusion of the peptides into the ganglion. In preparations with a pyloric cycle frequency $>$1.3 Hz in saline, both *ion*s and one *son* were cut to reduce modulatory input coming from the CoGs and projecting into the STG [11], because it is known for *C. borealis* that the effects of some Dip-ASTs depend on the pyloric frequency in saline [60]. The extracellular recordings of the motor nerves were performed with a pair of stainless steel wire electrodes, one of which was placed next to the nerve and isolated from the bath with Vaseline. The other electrode was placed in the bath. Data were collected on a chart recorder (Dash IV, Astro-Med, West Warwick, RI, USA). Preparations were continuously superfused (1–4 ml/min) with saline and the bath volume was 5 to 8 ml. Stock solutions of 10^{-3} M synthetic Dip-AST III (Bachem Biochemicals, Heidelberg, Germany) and 10^{-3} M of the synthetic crayfish allatostatin-like peptide in distilled water were diluted to the final concentration just before superfusion.

3. Results

3.1. Immunocytochemistry and EIA

The entire CNS, the STNS, and the pericardial organs of the crayfish *O. limosus* contain ASTir neuronal structures. In the eyestalk, strongly staining ASTir fiber networks are detected in the medullae externa, interna, and terminalis but not in the lamina ganglionaris (Fig. 1a). The stratified ASTir fibers in the medullae externa and interna arise from >100 small cortical cell bodies and three smaller unidentified clusters around these neuropils. Another four cell clusters scattered around the cortex of the medulla terminalis give rise to a complex innervation of almost all subfractions of this neuropil together with fibers entering from the brain via the protocerebral tract. The neurohemal sinus gland contains a few tiny fibers of faint immunoreactivity and of unknown origin (labeling did not occur in all preparations). In the brain, all delineated protocerebral, deutocerebral, and tritocerebral neuropils contain strongly stained fiber plexuses with prominent concentrations in the anterior and posterior protocerebral neuropils, the so-called optic neuropils, the central body, the accessory and olfactory lobes, and the antennary neuropils (Fig. 1b and c). The central body receives inputs from the anterior median cell cluster, and the accessory lobe glomeruli are almost exclusively innervated by several hundred small globuli cells (cluster 9, see Sandeman et al. [56]; Fig. 1b and c). Fibers in the antennary (II) neuropils partly originate in ventral median and posterior median somata clusters. Several unidentified tracts and commissures in the brain contain ASTir fibers, but the olfactory–globular tract linking the brain olfactory centers and hemiellipsoid bodies of the eyestalk is essentially devoid of ASTir fibers. However, the brain olfactory neuropils contain sparsely distributed fine fiber plexuses (Fig. 1c). The connective ganglia contain three clusters of three to six small cells and about four to five cells with larger, strongly stained somata, all of which branch in the neuropil of these ganglia (Fig. 1d). The superior (*son*) and inferior (*ion*) esophageal nerves contain at least two and four fibers, respectively, which connect the connective ganglia neuropils with the peripheral STNS. Part of the fibers in the *ion* as well as two of four fibers in the inferior ventricular nerve (*ivn*) arise from two strongly stained somata in the esophageal ganglion (Fig. 1e). The inferior ventricular nerve fibers branch profusely in the brain. The inputs of fibers into the immunostained neuropil inside the STG originate from the connective ganglia entering via the *ion*, from up to four fibers in the dorsal ventricular nerve (*dvn*) and from up to maximally six intrinsic ganglion cells, one of which usually stains more strongly than the others (Fig. 1f). Each neuromer of the ventral nerve cord ganglia contains lateral or anterior lateral somata clusters as well as a varying number of cells in medial ventral positions. Part of the anterior lateral clusters (about 20–40 cell bodies) in the subesophageal and thoracic ganglia show central and peripheral innervation patterns (Fig. 1g and h). Most prominent are projections into the walking legs in the thorax and to plexuses of varicose fibers and terminals in extensive neurohemal release sites in the dorsal perineural sheath of the subesophageal and thoracic ganglia, in the perineurium of the dorsal nerve roots (roots 2 and 3) of the corresponding neuromers (Fig. 1g and h) and in the neurohemal pericardial organs that are innervated via the segmental nerves (Fig. 1h and j). In the pericardial organs, which, in crayfish, are a composite of subesophageal and thoracic segmental nerves anastomosing by longitudinal trunks after having entered the pericardial cavity, almost all parts contain varicose fiber arborizations and typical neurohemal terminals next to the surface of these structures (Fig. 1j). More sparsely distributed are ASTir neurons in the abdominal ganglia. Apart from anterior lateral clusters of three to four cells, up to six ventral median cells can be detected in each ganglion, which contribute to extensive neuropilar fiber networks (Fig. 1i). However, none of these cells shows peripheral projections. This also holds true for the fused terminal ganglion, from which the innervation of the hindgut arises; no immunolabeling was seen in efferent axons, although neuronal processes in the neuropil of this ganglion were labeled, and hindgut tissues were devoid of AST immunoreactivity.

The distribution of ASTir neuronal structures correlates well with our quantitative evaluation of ASTir material extractable from central nervous tissues of the crayfish *O. limosus* with the newly developed Dip-AST I EIA (Fig. 2). The ED_{50} value for the detection of Dip-AST I standard in our assay is ≈6.25 fmol Dip-AST I per well (= concentration of 62.5 pM; detection limit, ≈10 pM), but the cross-reactivity of the identified crayfish ASTir peptides (see below) was <1%. The largest amounts of ASTir material were found in the eyestalk and the subesophageal and thoracic ganglia. The latter ganglia always included considerable parts of the segmental nerves between the cuts through the connectives.

3.2. Peptide isolation and identification

Four to five HPLC purification steps were necessary for the identification of three ASTir peptides of the crayfish *O. limosus*, as shown in Fig. 3. The immunopositive fractions at 55 and 56 min of retention time (24.7% and 25.0% MeCN, respectively; see box I in Fig. 3a) from the first HPLC run were subjected to a different column that separated immunopositive fractions at 21 and 22 min (21.0% and 21.2% MeCN, respectively; Fig. 3b). From these pooled fractions, two different areas of ASTir peptides were separated in the third HPLC step, which yielded two immunopositive major fractions at 41.9 min (23.3% MeCN) and 46.0 min (29.7% MeCN), respectively (Fig. 3c). The first of these immunopositive fractions was purified in the fourth HPLC step, and we obtained a large peak of reasonable homogeneity at 33.2 min (30.6% MeCN; Fig. 3e), which could be subjected without further purification to mass spec-

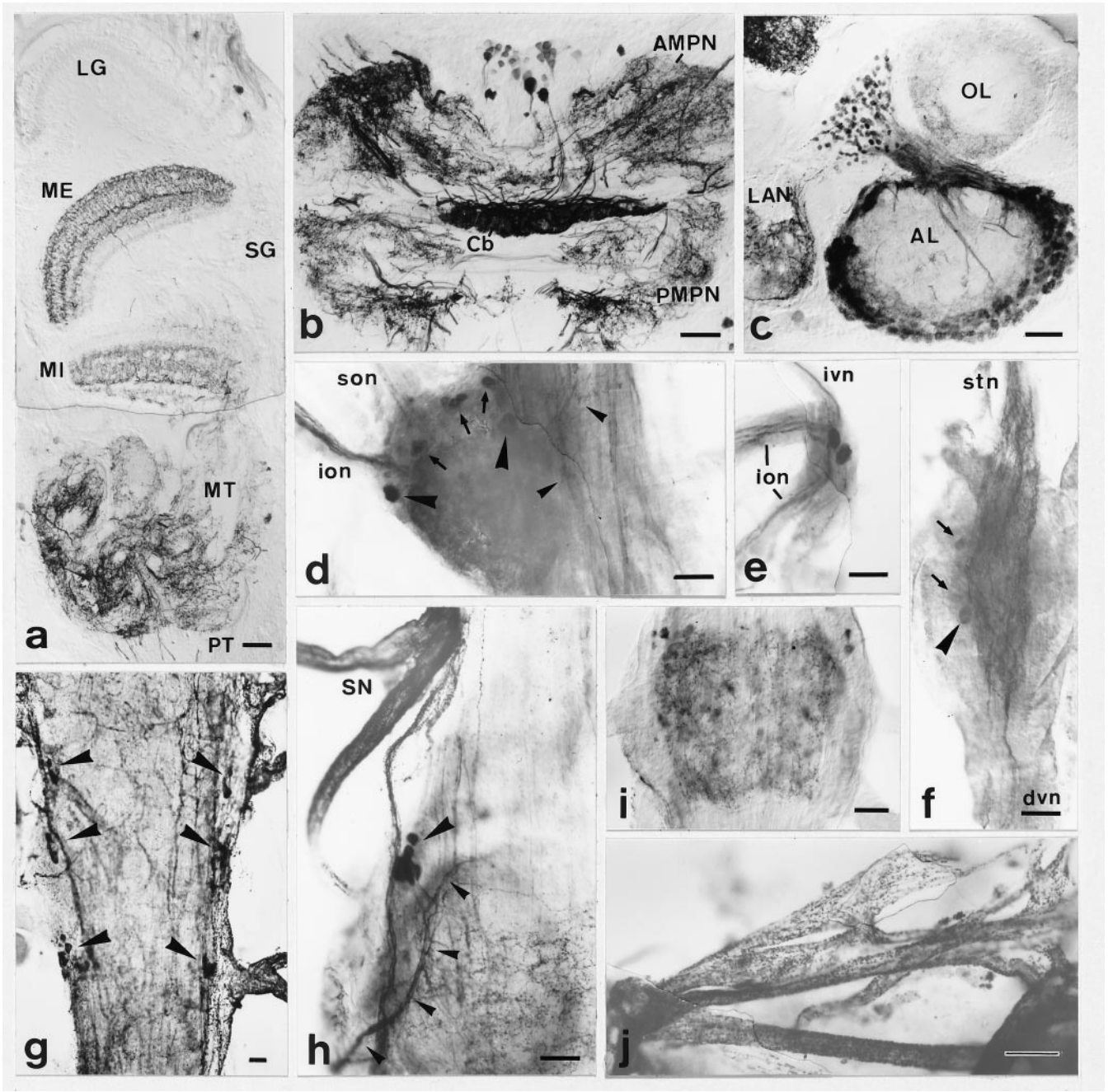

Fig. 1. Distribution of allatostatin-like immunoreactive (ASTir) neurons in Vibratome sections (50 μm; a–c) and whole mount preparations (d–f) of the central and peripheral nervous system of the crayfish *Orconectes limosus*. (a) Eyestalk ganglia showing ASTir fiber networks in the medullae externa, interna, and terminalis (ME, MI, and MT) but not in the lamina ganglionaris (LG), and fibers connecting to the brain via the protocerebral tract (PT). (b) Dense fiber networks in the anterior and posterior median protocerebral neuropils (AMPN and PMPN) and the central body (Cb) partially arising from somata in the anterior median cell cluster of the brain. (c) Olfactory centers of the brain showing globuli cells innervating the accessory lobe (AL) and networks of fine fibers in the olfactory lobe (OL) and the lateral antennary neuropil (LAN). (d) Groups of small (arrows) and large cell bodies (large arrowheads) and fibers in the superior and inferior esophageal nerves (*son* and *ion*) and at the surface of the ganglion (small arrowheads). (e) Two strongly stained cell bodies in the esophageal ganglion giving rise to fibers in the *ion* and in the inferior ventricular nerve (*ivn*). (f) Stomatogastric ganglion showing dense neuropilar fiber networks partially arising from strongly (arrowhead) and faintly staining (arrows) ASTir intrinsic cells. Note unstained neurons in the vicinity. (g) Somata clusters in the subesophageal ganglia (arrowheads) partially giving rise to extensive networks of varicose fibers and terminals at the surface of the segmental nerve roots and neurohemal areas in the perineurium. (h) Anterior lateral cell cluster in the left half of a third thoracic ganglion showing T-shaped branches (arrowheads) leading to leg innervations and the supply of the segmental nerve roots (SN). (i) Anterior lateral cell bodies and neuropil fibers in the third abdominal ganglion, ventral cells out of focus. (j) Trunks in the pericardial organs showing extensive networks of varicose fibers and terminals next to the surface of the organ. Scale bars, 100 μm.

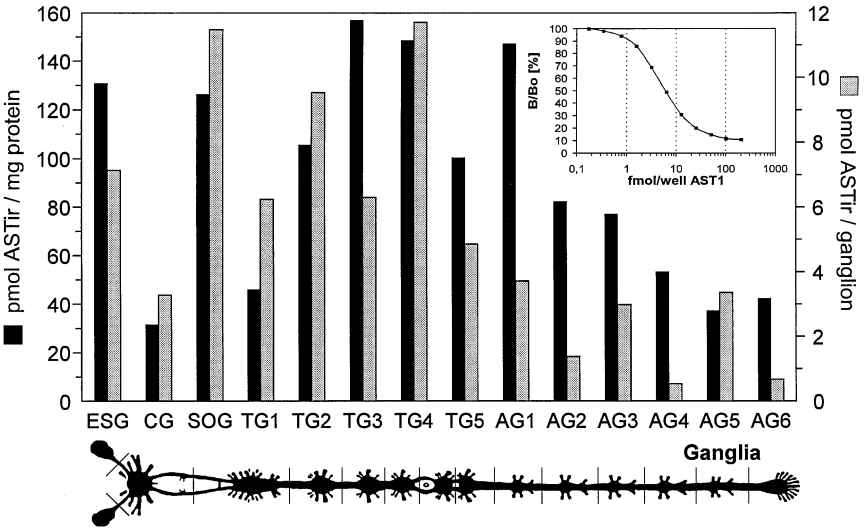

Fig. 2. Quantitative distribution of allatostatin-like immunoreactive (ASTir) peptides in the central nervous system (CNS) of the crayfish *O. limosus* (lines in the CNS sketch indicate connective transsections), expressed as pmol ASTir/mg protein (black columns) and ASTir per ganglion (stippled columns). Inset shows a typical standard curve for *D. punctata* allatostatin I (Dip-AST I). ESG, eyestalk ganglia; CG, cerebral ganglia; SOG, subesophageal ganglia; TG, thoracic ganglion; AG, abdominal ganglion.

trometry and microsequencing. MALDI-TOF analysis on two different machines resulted in a molecular ion detected at 795.2 Da ($M + H^+$; Table 1), consistent with the results of unambiguous Edman sequencing of an octapeptide of the sequence AGPYAFGL(amide) with a calculated mass of 794.93 Da (as $M + H^+$ ion; Table 1). This sequence is identical to that of the previously described carcinustatin 8 (CST 8) of the shore crab, *C. maenas* [19]. However, further purification of the small ASTir peak fraction eluting just before CST 8 in the same run (arrow in Fig. 3e) yielded a novel peptide eluting as a single ASTir peak fraction at 20.4 min (23.5% MeCN) in the fifth run (Fig. 3f). MALDI-TOF analysis of this peak fraction resulted in molecular peptide ions detected at 882.5 Da ($M + H^+$) and ions of its sodium and potassium adducts (Table 1). The mass of this major peptide ion was consistent with the results of Edman sequencing of a nonapeptide of the sequence SAGPYAFGL-(amide) with a calculated mass of 882.01 Da (as an amidated $M + H^+$ ion; Table 1). This novel peptide, termed orcostatin I (OST I), is obviously an analogon of CST 8, N-terminally extended by a serine residue. Further analysis of post-source-decay spectra revealed N-terminal fragment ions consistent with the sequence of OST I (Table 1). The second fraction at 47 min of the third run yielded two major ASTir fractions in the fourth step HPLC (Fig. 3d). The last one of these eluting at 27.5 min (30.7% MeCN) was purified further in a fifth step HPLC to yield a single ASTir peak at 18 min (26% MeCN; Fig. 3g). MALDI-TOF analysis of this peak fraction resulted in molecular peptide ions detected at 908.8 Da ($M + H^+$) in the linear mode, but in the reflectron mode in an ion at 907.6 Da ($M + H^+$) and a pronounced ion of its sodium adduct at 929.9 Da (Table 1). The mass of the peptide ions fits the results of Edman sequencing obtained for the novel octapeptide of the sequence PRVYGFGL-(amide), termed orcostatin II (OST II), with a calculated mass of 908.09 Da (as an amidated $M + H^+$ ion; see also Table 1). post-source-decay spectra analysis revealed N-terminal fragment ions consistent with the sequence of this novel peptide (Table 1), which shares only the tyrosine in the fourth position and the C-terminal FGLamide with the other two peptides. Comparison of elution patterns of the small lots of the native *O. limosus* CST 8 and orcostatins that remained after mass determination and sequencing with those of the synthetic peptides in amidated form confirmed the identity of the peptides. In each case, both the native and the synthetic peptides eluted at exactly identical retention times (Fig. 4a–f). Thus, we can assign the following primary structures of AGPYAFGL-NH_2 as identical to CST 8 described previously [19], SAGPYAFGL-NH_2 to OST I, and PRVYGFGL-NH_2 to OST II, respectively.

3.3. Muscle bioassays

Application of CST 8 on spontaneously active hearts and hindguts of *O. limosus* resulted, only in the cases of hindguts, in a decrease in both the amplitude and frequency of myogenic contractions. The heartbeat performance was virtually unaffected by CST 8 (data not shown). The inhibitory effects on frequency and amplitude of the hindgut contractions were reversible after washing with saline, which, however, could take several minutes. Similar inhibitory effects on the crayfish hindgut were observed for OST I and OST II. Although it is difficult to quantify inhibition of spontaneous activity, examination of the recorded traces (control frequencies, 29.2 ± 5.1 contractions per min; $n = 98$) revealed in several experiments that the inhibitory effects of all peptides were dose dependent and of almost equal strength, with a threshold between 10^{-9} and 10^{-8} M and a

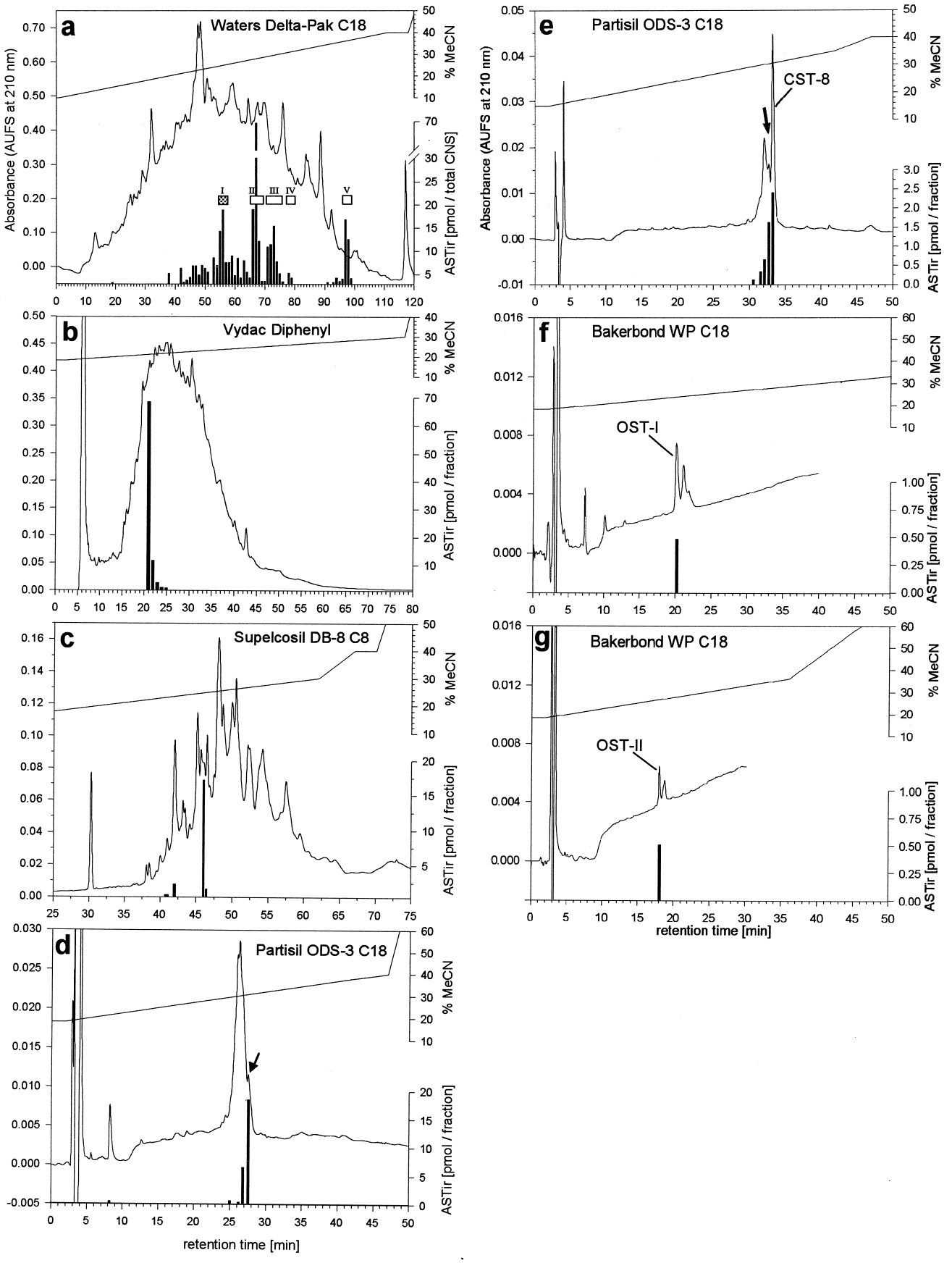
a
Waters Delta-Pak C18
b
Vydac Diphenyl
c
Supelcosil DB-8 C8
d
Partisil ODS-3 C18
e
Partisil ODS-3 C18
CST-8
f
Bakerbond WP C18
OST-I
g
Bakerbond WP C18
OST-II
Absorbance (AUFS at 210 nm)
% MeCN
ASTir [pmol / total CNS]
ASTir [pmol / fraction]
retention time [min]

Table 1
Amino acid sequences and molecular masses of crayfish allatostatin-like peptides and their N-terminal fragments as determined by MALDI time-of-flight and post-source-decay analyses

Peptide	Sequence	M_r Calculated			M_r Measured			
		$[M + H^+]$ Average	$[M + Na^+]$ Average	$[M + K^+]$ Average	$[M+ H^+]$ Lin. Mode	$[M + H^+]$ Refl. Mode	$[M + Na^+]$ Refl. Mode	$[M + K^+]$ Refl. Mode
CST 8	AGPYAFGLa[a]	794.93	816.91	833.02	795.2[a]	—	817.1[a]	833.3[a]
	AGPYAFGLa	794.93	816.91	833.02	795.2	—	816.5	832.5
OST I	SAGPYAFGLa	882.01	903.99	920.09	882.5	—	904.0	919.8
OST II	PRVYGFGLa	908.09	930.07	946.18	908.8	907.6	929.9	—
OST I fragments (b-ions)								
	SAGPYAFG	751.80				752.1		
	SAGPYAF	694.75				695.2		
	SAGPYA	547.57				547.9		
	SAGPY	476.49				476.4		
	SAGP	313.32				313.6		
	SAG	216.20				216.1		
OST II fragments (b-ions)								
	PRVYGFG	777.89				778.4[b]		
	PRVYGF	720.84				721.3[b]		
	PRVYGF(-NH_3[c])	703.81				704.3		
	PRVYG	573.66				573.8		
	PRVYG(-NH_3[c])	556.63				556.7		
	PRVY	516.61				516.3		
	PRV	353.43				353.9		
	PRV(-NH_3[c])	336.41				336.7		

[a] Data obtained by the first MALDI-MS system.
[b] Data represent maxima of small peaks in the PSD spectrum.
[c] Data for b-fragment ions lacking one amino group.
MALDI, matrix-assisted laser desorption/ionization; CST, carcinustatin; OST, orcostatin; MS, mass spectrometry.

maximum at 10^{-6} M, at which concentration in several cases complete inhibition was observed. The effect lasted 10 to 15 min, after which the spontaneous activity slowly came back to normal conditions as exemplified in Fig. 5. We restricted, however, our measurements to the maximum effects usually appearing between 1 and 5 min after sample application for the construction of dose-response curves (Fig. 6) showing that frequency and amplitude of contractions are almost equally affected. Significant inhibition ($P < 0.05$), compared with the control of frequencies and amplitudes of contractions, was obtained at a concentration of 10^{-8} M for all three peptides.

In the cockroach hindgut assay, CST 8 (10^{-10} to 10^{-7} M) had no effect on the spontaneous activity or on contractions induced by proctolin added at 10^{-8} or 10^{-9} M (data not shown). However, when we stimulated contractions in the hindgut by adding *M. sexta* allatotropin at 10^{-7} M to the organ bath, the addition of synthetic CST 8 exerted a strong and dose-dependent inhibition of peptide-stimulated contractions ($n = 3$) with a threshold at $\approx 10^{-9}$ M (Fig. 7).

3.4. Electrophysiology

A series of experiments was performed to test the physiological action of CST 8 on the pyloric motor pattern generated by the STG and compare its effect with that of Dip-AST III in two crustacean species, the crab *C. pagurus* and the crayfish *C. destructor*. The pyloric motor pattern involves alternating bursts of activity in three different types of motor neurons, lateral pyloric, pyloric, and pyloric dilator neurons. The pyloric rhythm was monitored by extracellular recordings from the dorsal ventricular nerve (*dvn*) as shown in the top right sketch of Fig. 9. In five experiments on *C. pagurus*, both CST 8 [Fig. 8 (left)] and Dip-AST III [Fig. 8 (right)] caused a very similar decrease in the pyloric cycle

←

Fig. 3. High-performance liquid chromatography (HPLC) purification of allatostatin-like immunoreactive (ASTir) peptides of the crayfish *O. limosus* as determined in fractions by using the *D. punctata* allatostatin I (Dip-AST I) enzyme immunoassay. (a) First step HPLC of CNS material on a Waters Delta-Pak C18 cartridge showing three dozen ASTir fractions some of which exhibit strong immunoreactivity (boxes I to V). (b) Second-step HPLC purification of pooled fractions eluted at 55 and 56 min from box I (in a) yielding two strongly ASTir fractions at 21 and 22 min. (c) Third-step HPLC purification of the pooled fractions from (b) yielding two ASTir fraction areas at 42 min and ≈47 min; only the relevant part of the chromatogram is shown. (d) Rechromatography of the 47-min fraction in (c) yielding two major ASTir fractions (arrow indicates fraction rechromatographed in g). (e) Last step for the HPLC purification on a Partisil ODS-3 C18 column of the fraction eluted at 41.9 min in (c) yielding carcinustatin 8 (= CST 8) in the largest peak fraction eluted at 33.5 min (arrow indicates fraction rechromatographed in f). (f) Rechromatography of the fraction indicated in (e) yielding one ASTir peak fraction (arrow) containing orcostatin I (OST I). (g) Rechromatography of the fraction indicated in (d) yielding one ASTir peak fraction (arrow) containing orcostatin II (OST II).

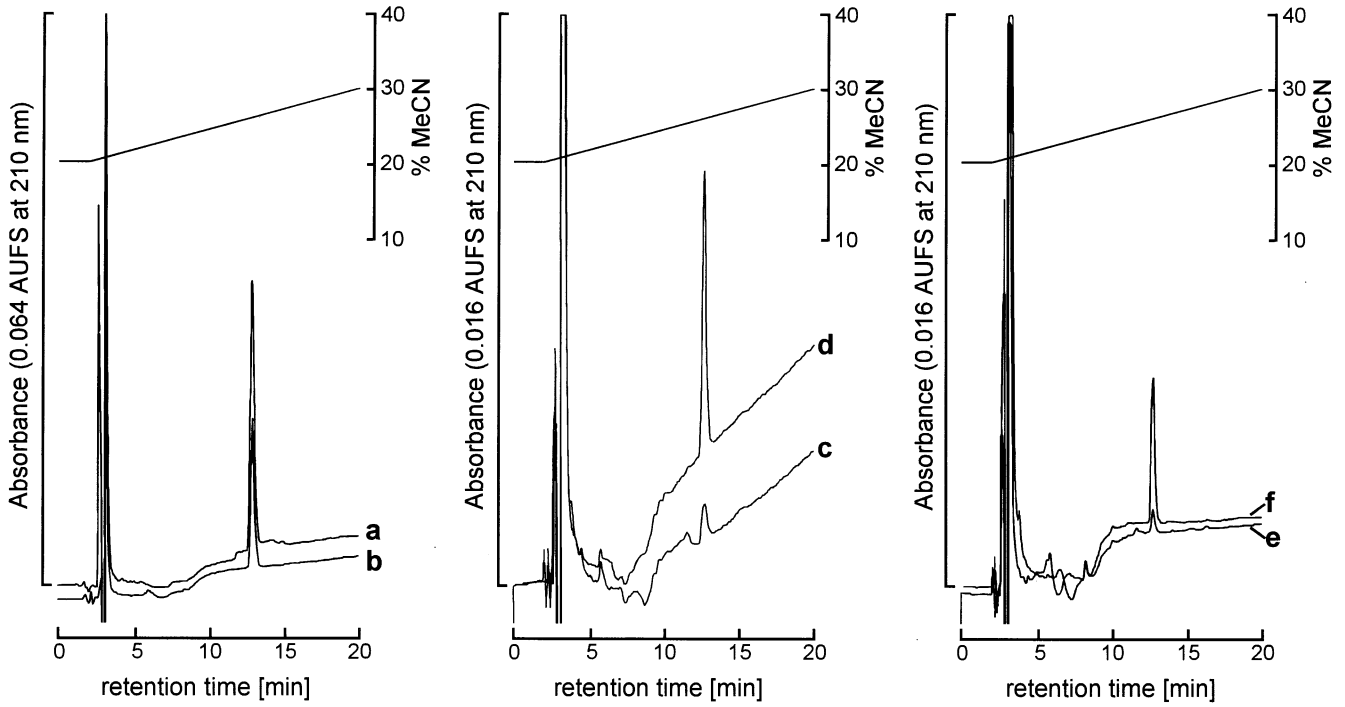

Fig. 4. High-performance liquid chromatographs of ≈250 pmol of native (a) and 150 pmol of synthetic crayfish carcinustatin 8 (b), ≈15 pmol of native (c) and 100 pmol of synthetic crayfish orcostatin I (d), ≈10 pmol of native (e) and 100 pmol of synthetic crayfish orcostatin II (f). The comparative runs were performed directly one after another at the same chromatographic conditions on an analytical Bakerbond C18 column; gradient elution from 20.4% to 32.4% aqueous acetonitrile (MeCN) containing 0.1% trifluoroacetic acid in 25 min at a flow rate of 1 ml/min. Each pair of peptides eluted at exactly the same retention times, thus confirming the identity of the peptides.

frequency, which was reversible. At a concentration of 10^{-7} M, CST 8 reduced the frequency from 0.76 Hz in saline to 0.61 Hz, and Dip-AST III from 0.79 Hz in saline to 0.65 Hz.

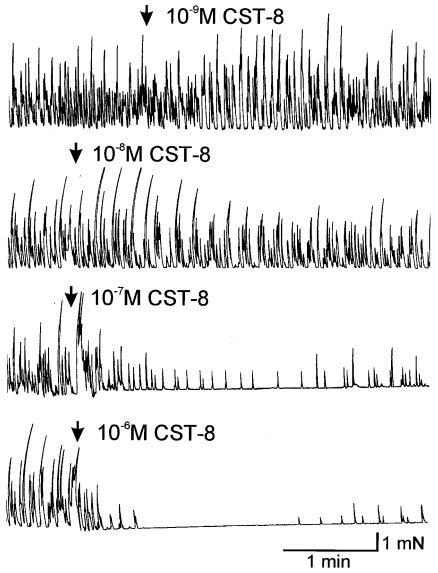

Fig. 5. Mechanograms showing the dose-dependent inhibitory actions of synthetic crayfish carcinustatin 8 (CST 8) on a spontaneously active hindgut of the crayfish *O. limosus*. Note the complete inhibition of contractile activity at a concentration of 10^{-6} M carcinustatin 8 lasting several minutes.

At a concentration of 10^{-6} M, CST 8 reduced the frequency from 0.78 Hz in saline to 0.37 Hz and Dip-AST III reduced the frequency from 0.83 Hz in saline to 0.51 Hz. In most preparations, control patterns of activity returned after 10 to 20 min of washing with saline.

To determine the dose dependence of the CST 8 effect, five experiments were performed on the crab *C. pagurus* by applying CST 8 from 10^{-9} to 10^{-6} M to the bath. At concentrations of 10^{-9} or 10^{-8} M CST 8, the frequency of the pyloric rhythm either increased ($n = 5$) or decreased ($n = 5$) slightly. The results of one such experiment is shown in Fig. 9, where 10^{-9} M CST 8 reduced the frequency from 0.72 Hz in saline to 0.65 Hz and 10^{-8} M increased the frequency from 0.70 Hz in saline to 0.73 Hz. In all five experiments, however, CST 8 caused a decrease in the frequency of the pyloric rhythm at concentrations of 10^{-7} and 10^{-6} M CST 8. In this particular experiment, 10^{-7} M CST 8 reduced the frequency from 0.76 Hz in saline to 0.61 Hz, and 10^{-6} M reduced the frequency from 0.78 Hz in saline to 0.37 Hz. The percent change in pyloric cycle frequency produced by a given concentration of peptide varied from preparation to preparation, depending on the initial control frequency; i.e. 10^{-6} M CST 8 had pronounced inhibitory effects when the preparations were slowly cycling but only weak effects on preparations with faster pyloric rhythms (Fig. 10).

We also compared the actions of CST 8 and Dip-AST III

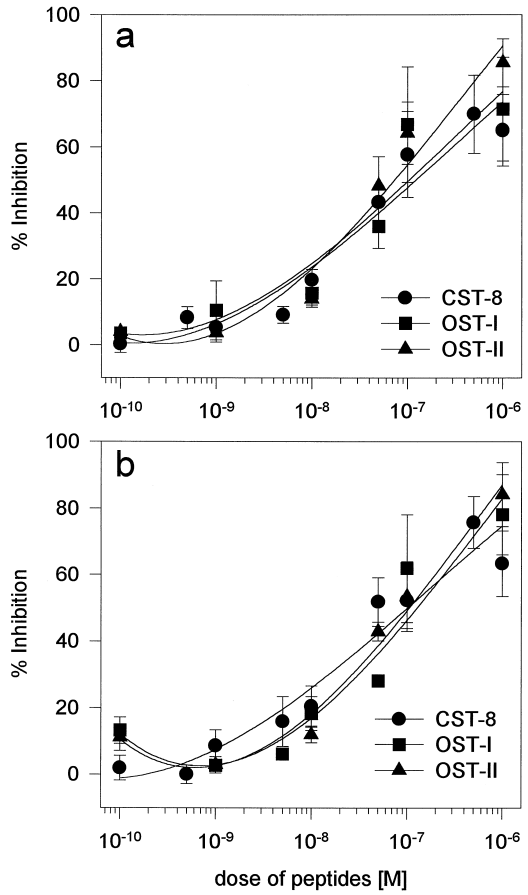

Fig. 6. Dose-response curves showing the inhibitory actions of carcinustatin 8 (CST 8) and orcostatins I and II (OST I and OST II) on the frequency (a) and amplitude (b) of contractions of semiisolated hindguts of the crayfish *O. limosus*. Data represent percentages of mean values after application divided by mean values (± standard error) before application of CST 8 ($n = 6$; circles), OST I ($n = 4$; squares), and OST II ($n = 4$; triangles). Significant inhibition compared with the control of frequencies and amplitudes of contractions occurs at concentrations higher than 5×10^{-9} M for all three peptides ($P < 0.05$).

on the pyloric rhythms of the crayfish *C. destructor* ($n = 5$). Both peptides exhibit the same effects at about the same concentration, and these effects were reversible in saline. The effects, however, were somewhat different from those seen in *C. pagurus*. Before reducing the cycle frequency, both CST 8 and Dip-AST III reduced the spike frequency of a neuron that fired between the lateral pyloric and the pyloric dilator bursts (Fig. 11). At a concentration of 10^{-7} M CST 8 [Fig. 11 (left)] or Dip-AST III [Fig. 11 (right)], the firing frequency of this neuron was clearly reduced, although the frequency of the pyloric rhythm was almost unchanged (saline, 0.48 Hz; 10^{-7} M CST 8, 0.50 Hz; saline, 0.48 Hz; 10^{-7} M Dip-AST III, 0.45 Hz). At a concentration of 10^{-6} M CST 8 [Fig. 11 (left)] or Dip-AST III [Fig. 11 (right)], the firing frequency of this unit was completely abolished. At these concentrations also the pyloric cycle frequency was reduced. CST 8 at 10^{-6} M reduced the frequency from 0.50 to 0.43 Hz, and Dip-AST III at 10^{-6} M from 0.46 to 0.33 Hz.

4. Discussion

Analysis of the wide distribution of ASTir peptides in immunocytochemically stained neuronal structures of the crayfish *O. limosus* revealed an enormous complexity comprising interneurons in almost all ganglia of the CNS as well as neurosecretory cells, especially in the ventral nervous system with projections in well-established large neurohemal organs. The topographic distributions of crayfish ASTir neurons largely match but to some extent exceed those described in several crayfish species, e.g. for neurons containing serotonin [25,53,57] or several native crustacean peptides such as red-pigment concentrating hormone [40], pigment-dispersing hormone [41], proctolin [58], FMRF-amide-related peptides [45], and crustacean cardioactive peptide (CCAP) [46,76]. Furthermore, the neuronal distribution of ASTir peptides in the STNS of *O. limosus* is very similar to those described for other astacuran and brachyuran crustaceans [59,60]. The distribution of ASTir neurons in the crayfish CNS matches the quantitative EIA determinations of immunoreactivity in different ganglia. Because the antibody to Dip-AST I used in the EIA is highly specific for Dip-AST I already when compared with other Dip-ASTs [54,82], it is not surprising that the cross-reactivity to crayfish CST 8 and orcostatins is quite low (<1%). However, this implies that the actual total amount of ASTir peptide in

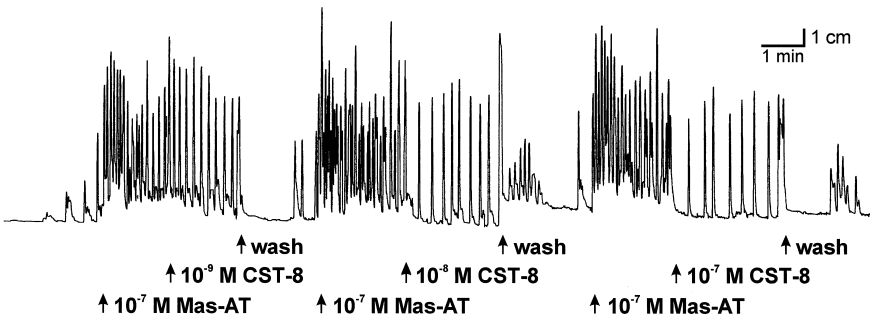

Fig. 7. Mechanogram showing the stimulatory effect of a *M. sexta* allatotropin (Mas-AT) and the inhibitory effect of synthetic crayfish carcinustatin 8 on the hindgut of the cockroach *L. maderae* (recorder swing-out in cm).

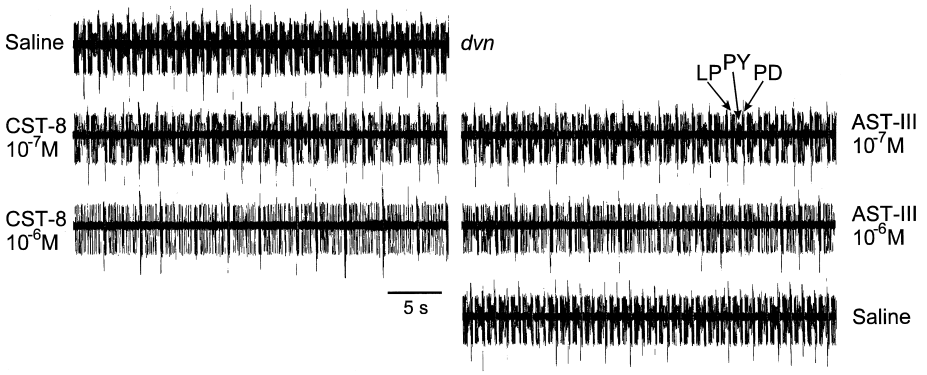

Fig. 8. Comparison of the effects of crayfish carcinustatin 8 (CST 8) and *Diploptera* allatostatin III (AST III) on the pyloric cycle frequency of the stomatogastric ganglion of the crab *C. pagurus*. Activity of lateral pyloric (LP), pyloric (PY), and pyloric dilator (PD) neurons was recorded extracellularly from the dorsal ventricular nerve (*dvn*). On the left are traces from dorsal ventricular nerve recordings before and 10 min after CST 8 application and on the right are the traces after 10 min of AST III application. At concentrations of 10^{-7} and 10^{-6} M, both CST 8 and AST III produced a noticeable decrease in the cycling frequency of the pyloric rhythm (saline, 0.76 ± 0.01 Hz; 10^{-7} M CST 8, 0.61 ± 0.03; 10^{-6} M CST 8, 0.37 ± 0.07 Hz; 10^{-7} M AST III, 0.65 ± 0.01 Hz; 10^{-6} M AST III, 0.51 ± 0.10 Hz; saline, 0.88 ± 0.01 Hz; mean ± SD; $n = 10$ periods).

the crayfish CNS is much higher than indicated by the EIA. Nevertheless, when judging from immunostainings of neurons and the matching quantities of peptide material, the widely distributed ASTir peptides most likely participate in neuromodulation in sensory (visual and olfactory) systems of the crayfish eyestalk and brain. The peptides can probably act in the control of several different motor systems, as has been shown here in the cases of the STG rhythmic motor outputs of a crayfish and a crab. The actions of crayfish CST 8 and the orcostatins on the hindgut, however, we consider to be of humoral origin, because no ASTir hindgut innervations have been observed. The existence of several more ASTir fractions after the first HPLC step suggests that a similar multitude of allatostatin-like peptide, as described recently for the crab [19], also exists in the crayfish, which is currently under investigation. CST 8 is

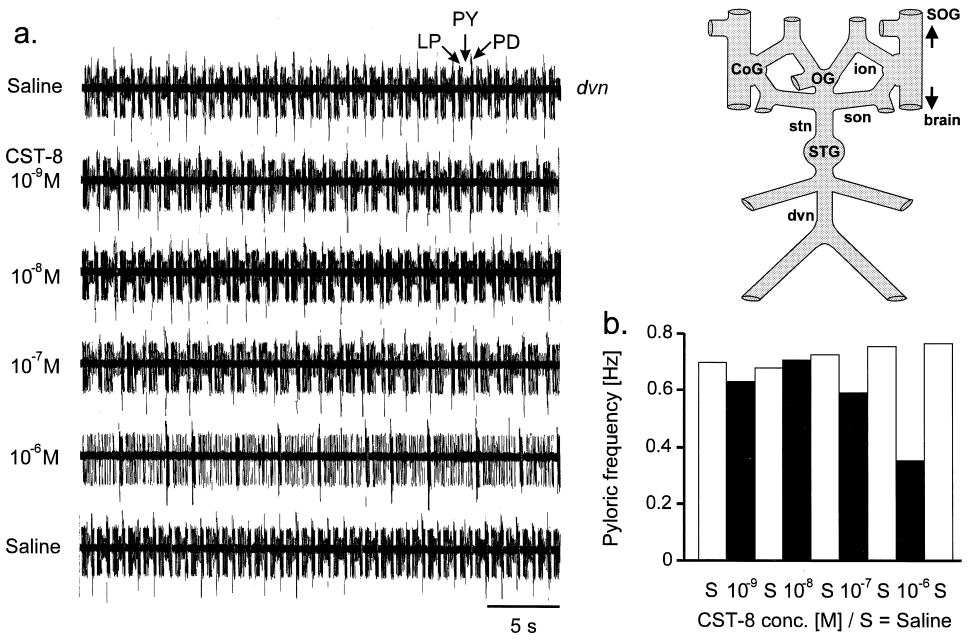

Fig. 9. Dose dependence of the carcinustatin 8 (CST 8) action on the pyloric rhythm of the crab *C. pagurus*. (a) Activity of lateral pyloric (LP), pyloric (PY), and pyloric dilator (PD) neurons was recorded extracellularly from the dorsal ventricular nerve (*dvn*) at 10^{-9}, 10^{-8}, 10^{-7}, and 10^{-6} M CST 8. (b) Histogram showing the change in pyloric cycle frequency after application of differing concentrations of CST 8 (black columns) relative to saline controls (white columns) before application or after the washes (saline, 0.72 ± 0.01 Hz; 10^{-9} M CST 8, 0.65 ± 0.02 Hz; saline, 0.70 ± 0.01 Hz; 10^{-8} M CST 8, 0.73 ± 0.03 Hz; saline, 0.76 ± 0.01 Hz; 10^{-7} M CST 8, 0.61 ± 0.03 Hz; saline, 0.78 ± 0.02 Hz; 10^{-6} M CST 8, 0.37 ± 0.07 Hz; saline, 0.79 ± 0.01 Hz; mean ± SD, $n = 10$ bursts; SD of all bars too small to show). Measurements were taken 10 min after bath application of CST 8 and 10 min after starting the wash. Inset shows a sketch of the combined preparation of ganglia and nerves (CoG, connective ganglion; *ion*, inferior ventricular nerve; OG, esophageal ganglion; SOG, subesophageal ganglion; *son*, superior esophageal nerve; STG, stomatogastric ganglion; *stn*, stomatogastric nerve).

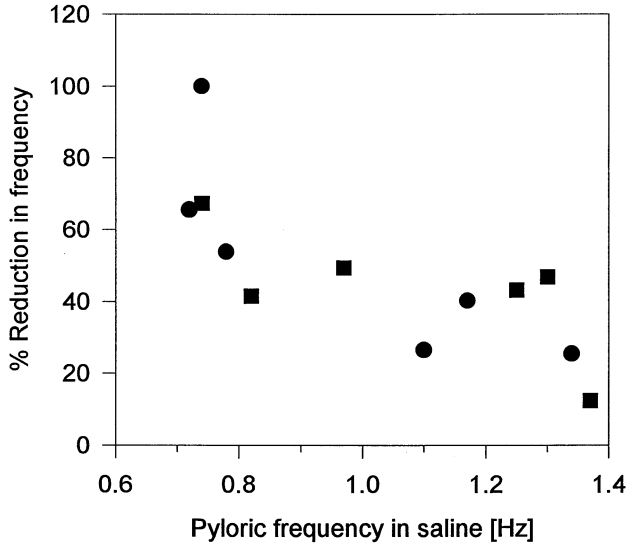

Fig. 10. Reduction of the pyloric cycle frequency in *C. pagurus* during individual applications of crayfish carcinustatin 8 (CST 8) and *Diploptera* allatostatin III (Dip-AST III) depends on the initial control frequency in saline. Pyloric cycle frequencies were measured from extracellular dorsal ventricular nerve recordings ($n = 5$) made before and 10 min after application of CST 8 (10^{-6} M; circles) or Dip-AST III (10^{-6} M; squares). In four of these five experiments, measurements were taken after cutting the *ion*s and one *son*, which caused a reduction of the control frequency. In one of these four experiments, CST 8 was also applied before the nerves were cut.

obviously a new example in crustaceans for exactly the same members of peptide families occurring across species borders. This was hitherto known only for orcokinins [8]. A higher degree of structural conservation is only known for important nonfamily peptides such as red-pigment concentrating hormone [26], proctolin [36], and CCAP [14] in crustaceans. It seems, therefore, unlikely, although not completely excluded, at present, that CST 8 may be a breakdown product of OST I, because enzymatic processing of prohormones of allatostatin-like peptides by so-called N-terminal trimming may release single residues or a dipeptide from the N-terminus of a larger peptide [22]. However, final decisions about this problem will have to await the unraveling of the prohormone structures of the orcostatins.

The hindgut of *O. limosus* responds to several crustacean myostimulatory factors such as CCAP [68,69] and orcokinin [67], but we provide here the first demonstration of native crustacean myoinhibitory factors, the identified crayfish CST 8 and OST I and OST II. The inhibitory effect is obvious and similar for all three peptides, although the complete inhibitions of hindgut contractility at higher concentrations are not long lasting, which may be indicative of a rapid breakdown of the peptides at the tissue level and a role in the fine tuning of contractions only. It is surprising, however, that crayfish CST 8, in contrast to CCAP [69], did not affect the heartbeat, although it seems to be released from the neurohemal pericardial organs. In preliminary experiments, we found that 10^{-7} M CST 8 blocks CCAP-evoked stimulations of the hindgut of *O. limosus* but not those elicited by proctolin, which are similar to the ones described previously for a 'proctolin-like peptide' in a different crayfish species [44]. The latter is intriguing because stimulatory effects of proctolin in assays of the cockroach *D. punctata* hindgut are known to be inhibited by Dip-AST I [38,39]. It is interesting, however, that the proctolin-stimulated hindguts of the cockroach *L. maderae* also did not respond to CST 8 application. The blowfly Leu-callatostatins also did not affect the spontaneous and proctolin-induced contractility of the *L. maderae* hindgut, but inhibited that of the foregut only [23]. On the other hand, we could show here that the stimulatory action of Mas-allatotropin on the *L. maderae* hindgut was subject to CST 8 inhibition. These Mas-allatotropin-induced muscle contractions are likely to involve only the muscles of the posteriorly located rectal pads, which are innervated by both Mas allatotropin–immunoreactive and Dip-AST I–immunoreactive nerve fibers (Rudwall AJ, Nässel DR, unpublished

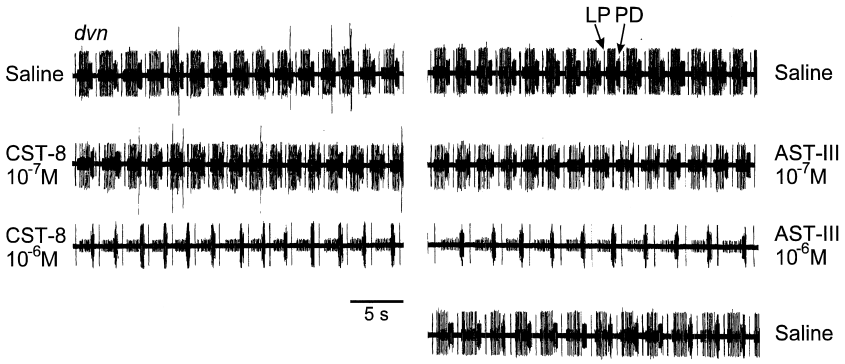

Fig. 11. Comparison of the effects of crayfish carcinustatin 8 (CST 8) and *Diploptera* allatostatin III (AST III) on the pyloric cycle frequency of the stomatogastric ganglion of the crayfish *C. destructor*. Traces from dorsal ventricular nerve recordings before and 10 min after application of CST (left) or AST III (right) showing for both peptides a reduction in the firing frequency of a neuron that fires action potentials between the lateral pyloric (LP) and pyloric dilator (PD) bursts. At a concentration of 10^{-6} M, both peptides produced a noticeable decrease in the cycling frequency of the pyloric rhythm (saline, 0.48 ± 0.04 Hz; CST 8 and CST 10^{-7} M, 0.50 ± 0.05 Hz; CST 8 and CST 10^{-6} M, 0.43 ± 0.04 Hz; saline, 0.48 ± 0.02 Hz; AST III 10^{-7} M, 0.45 ± 0.03 Hz; AST III 10^{-6} M, 0.33 ± 0.03 Hz; saline, 0.40 ± 0.03 Hz; mean ± SD, $n = 10$ periods). (For details on measurements and abbreviations, see Fig. 9).

data). Our experiments provide the first demonstration of a myostimulatory activity of an allatotropin on a cockroach hindgut. This peptide has previously been shown to be cardioacceleratory on semiisolated hearts of pharate adult *M. sexta* [80]. Although authentic CST 8 may not exist in *L. maderae,* the cross-phyletic bioactivity of the peptide implies that similarities must exist in the primary structures of CST 8 and peptides of this cockroach species that probably reside in the common C-terminus of these members of the allatostatin peptide family (see also below). The recent clarification of an AST-like tridecapeptide of *L. maderae*, in which the sequence of the 10 C-terminal amino acids is identical to that of Dip-AST I [47], provides further support for this view.

Several neuropeptides and other neuroactive compounds indicated by immunocytochemistry to be present in the STNS are known to change the motor pattern generated from the STG, when superfused onto an isolated STNS (for review, see Harris–Warrick et al. [27] and Marder et al. [43]). Electrophysiological investigations with insect neuropeptides in heterologous crustacean systems, have shown that some peptides have inhibitory effects and have paved the way for further identifications of novel classes of native crustacean neuromodulators. For instance, tests on the crayfish STNS with inhibitory cockroach peptides such as several Dip-ASTs [60] and leukomyosuppressin [74], the latter being the first inhibitory peptide identified in insects [31], gave first indications of the possible existence of inhibitory factors among the families of allatostatin-like and FMRF-amide-related peptides in arthropods other than insects. The electrophysiological results presented here provide the first evidence for the existence of direct physiological actions of a native crustacean allatostatin-like peptide, CST 8, on the STNS of *C. pagurus*. The actions are very similar to those of Dip-AST I to IV described for *C. borealis* [60] and another crayfish species, *C. destructor*. CST 8 and Dip-AST III require similar concentrations to inhibit the pyloric cycle frequency to about the same magnitude. CST 8 reduces the frequency of the pyloric rhythm in a dose-dependent manner and, similar to the Dip-AST III inhibition of the pyloric cycle frequency, the CST 8 inhibition is correlated with the initial frequency of the pyloric rhythm in saline. This particular correlation has been observed for several peptides; i.e. they have strong effects on the pyloric cycle frequency when bath-applied to preparations that were cycling at low frequencies, but have relatively little effect when applied to rapidly cycling preparations. The phenomenon is well known for peptides such as proctolin [33,42,50], FMRF-amide-related peptides [85], and tachykinin-related peptides [6], which increase the cycling frequency. It has been suggested that different hormonal or physiological states of the animal might cause the variability of the pyloric rhythms and their state dependence [50]. The physiological state was changed experimentally in most of the preparations by cutting the nerves (one *son* and two *ion*s) connecting the CoG with the STG. This operation obviously severs axons from modulatory input neurons, which have their somata in the CoGs and project to the STG [11]. Consequently, this initially increases the pyloric cycling frequency probably because of action potentials elicited by the cut, but is followed by a decrease in the frequency of the rhythms because of reduced modulatory inputs. Differences were found in the inhibitory effects produced by both CST 8 and Dip-AST III on the pyloric rhythms generated by the STG in the crayfish *C. destructor* compared with those observed in the crab *C. pagurus*. These differences might be related to the fact that an ASTir neuron is present in the STG of *C. destructor*, but not in *C. pagurus* [59,60].

In our experiments, CST 8 was bath-applied simultaneously onto all ganglia (CoGs, esophageal ganglion [OG], and STG). Therefore, we cannot yet distinguish whether the observed effects may be caused by: 1) inhibition of the excitatory inputs to the STG from neurons in the CoGs and the esophageal ganglion (OG) at the level of these ganglia or their STG terminals; 2) inhibition of cells of the pyloric network itself; or 3) both alternatives. When CST 8 or Dip-AST III was applied to a bath constructed around the STG only, the inhibitory effects on the pyloric rhythm were still present (data not shown). In *C. pagurus*, an increase in lateral pyloric burst duration was seen after allatostatin application in most experiments. This increase is not necessarily a direct effect of allatostatin, but could have resulted from the frequency reduction observed after nerve transsections. However, this demonstrates that allatostatin-like peptides must have at least some direct action on STG neurons or on presynaptic terminals of other excitatory inputs. Further experiments including intracellular recordings will be necessary to unravel the exact target cells for these peptides.

In insects, the conserved C-terminus of most allatostatins is required for the activity in vitro [51], whereas the N-terminus appears to confer the specificity and the affinity between the allatostatin peptides and their corresponding receptors [4,28,52]. The similarity of the effects of CST 8, the orcostatins, and Dip-AST III suggests that in crustaceans a conserved C-terminal Y**X**FGL-NH_2 is necessary for the bioactivity as well. It is noteworthy that all hitherto identified crab [19] and crayfish allatostatin-like peptides differ in primary structure from the >50 known insect allatostatins. However, among the cockroach allatostatins tested previously on the *C. borealis* STNS, only one (Dip-AST II, GDGRL**YAFGL-NH_2**) shows similarities in primary structure to CST 8 (AGP**YAFGL-NH_2**) with regard to the five C-terminal amino acids but was slightly less effective than Dip-AST III (GGSL**YSFGL-NH_2**; [60]), a peptide with even fewer similarities to CST 8. This may indicate that putative receptors conveying the observed actions of allatostatins and CST 8 hitherto examined in these crustacean species do not distinguish much between peptides sharing more than the **YXFGL-NH_2** residues at the C-terminus. The close similarities of actions of the different crayfish allatostatin-like peptides on the hindgut contractility further

support this view. From structure–activity studies on the inhibition of juvenile hormone biosynthesis by the octapeptide Dipstatin 4 and the octadecapeptide Dipstatin 2, it is known that the most important conserved core sequence is the **YXFGL**-NH_2 for interaction with probably two different receptors in the corpora allata [28,52]. Whereas the amino acid at the 'X' position is obviously of minor importance if not replaced by a D-amino acid, the Gly residue seems to be responsible for a possibly important C-terminal β-turn structure of allatostatins [28]. This differs from the observations on the specificity of the antibodies used in the present and previous studies indicating that the pre- and posttyrosyl amino acids are important epitopes for recognition by the antibodies [54,82] but not by the receptor(s).

Among the identified peptides, CST 8 is of special interest from a comparative point of view because this particular peptide occurs with the same sequence in the crab *C. maenas* [19]. Thus, it seems reasonable to assume that the same peptide may also occur in the crab and crayfish species used for our heterologous assays, which, however, has to await final proof from biochemical identification. Closely related members of the same peptide family can elicit similar changes in the motor pattern generated by the STG as is known for the adipokinetic hormone/red-pigment concentrating hormone peptide family [49], the FMRFamide-related peptides [85], and the tachykinin-related peptides [6,9]. In crustaceans, the tachykinin-related peptides are hitherto known to occur only in interneurons, whereas members of the other families also occur in typical neurosecretory neurons, a similar situation we meet with the orcostatins. Thus, for a putative family of crustacean allatostatin-like peptides now known for a crab [19] and a crayfish, we must consider both the neuromodulatory and the myomodulatory functions, the latter, in the case of the crayfish hindgut, obviously being brought about by allatostatin-like peptides of humoral origin. Future studies must unravel whether the entire multitude of allatostatin-like peptides of one species occurs in and is coreleased from the same ASTir neurons. If so, it remains to be determined whether peptide-specific differentiations of actions on targets in peripheral organs and several neuronal networks or a fine tuning of such targets by several similar peptides released from the same ASTir neurons prevail.

Acknowledgments

The authors thank Dr Simon G. Webster, University of Wales, Bangor, UK, and Barbara Reichwein and Susanne Weese at Bonn for carrying out valuable amino acid analyses. Thanks are due to Dr Chris Weise for help with automated Edman sequencing, Dr Peter Franke for carrying out the mass spectrometry, and Dr Sabine Schäfer for her help with STG electrophysiology at Berlin. Anne Karlsson at Stockholm is thanked for performing the cockroach hindgut assays. Supported by the German Academic Exchange Service (DAAD to H.D.), Deutsche Forschungsgemeinschaft (DFG, SFB 515 to P.S.), and the Swedish Natural Science Research Council (NFR to D.R.N.).

References

[1] Abel B, Dircksen H, Agricola H. Allatostatin-immunoreactive systems in the central and peripheral nervous system of crustaceans. Verh Dtsch Zool Ges 1994;87:3.

[2] Agricola HJ, Bräunig P. Comparative aspects of peptidergic signaling pathways in the nervous systems of arthropods. In: Breidbach O, Kutsch W, editors. The nervous systems of invertebrates: an evolutionary and comparative approach. Basel: Birkhäuser Verlag, 1995. pp. 303–27.

[3] Atherton E, Fox H, Harkiss D, Logan CJ, Sheppard RC, Williams BJ. A mild procedure for solid phase peptide synthesis: use of fluorenylmethoxy-carbonyl-amino acids. J Chem Soc Chem Commun 1978; 1978:537–9.

[4] Bendena WG, Garside CS, Yu CG, Tobe SS. Allatostatins: diversity in structure and function of an insect neuropeptide family. Ann NY Acad Sci 1997;814:53–66.

[5] Bennett HPJ, Browne CA, Goltzman D, Solomon S. Isolation of peptide hormones by reversed-phase high pressure liquid chromatography. In: Gross E, Meienhofer J, editors. Peptides: structure and biological function. Rockford, IL: Pierce Chemical Co, 1974. pp. 121–4.

[6] Blitz DM, Christie AE, Marder E, Nusbaum MP. Distribution and effects of tachykinin-like peptides in the stomatogastric nervous system of the crab, *Cancer borealis*. J Comp Neurol 1995;354:282–94.

[7] Böhm H, Hinterkeuser S, Heinzel H-G. Influence of neuropeptides on the feeding-behaviour of crayfish. Zoology 1998;101(suppl I):45.

[8] Bungart D, Hilbich C, Dircksen H, Keller R. Occurrence of the myotropic neuropeptide orcokinin in the shore crab, *Carcinus maenas*: evidence for a novel neuropeptide family. Peptides 1995;16:67–72.

[9] Christie AE, Lundquist CT, Nässel DR, Nusbaum MP. Two novel tachykinin-related peptides from the nervous system of the crab *Cancer borealis*. J Exp Biol 1997;200:2279–94.

[10] Christie AE, Skiebe P, Marder E. Matrix of neuromodulators in neurosecretory structures of the crab *Cancer borealis*. J Exp Biol 1995;198:2431–9.

[11] Coleman MJ, Nusbaum MP, Cournil I, Claiborne BJ. Distribution of modulatory inputs to the stomatogastric ganglion of the crab, *Cancer borealis*. J Comp Neurol 1992;325:581–94.

[12] Davis NT, Veenstra JA, Feyereisen R, Hildebrand JG. Allatostatin-like-immunoreactive neurons of the tobacco hornworm, *Manduca sexta*, and isolation and identification of a new neuropeptide related to cockroach allatostatins. J Comp Neurol 1997;385:265–84.

[13] Ding Q, Donly BC, Tobe SS, Bendena WG. Comparison of the allatostatin neuropeptide precursors in the distantly related cockroaches *Periplaneta americana* and *Diploptera punctata*. Eur J Biochem 1995;234:737–46.

[14] Dircksen H. Conserved crustacean cardioactive peptide (CCAP) neuronal networks and functions in arthropod evolution. In: Coast GM, Webster SG, editors. Recent advances in arthropod endocrinology. Cambridge: Cambridge University Press, 1998. pp. 302–33.

[15] Dircksen H, Homberg U. Crustacean cardioactive peptide-immunoreactive neurons innervating brain neuropils, retrocerebral complex and stomatogastric nervous system of the locust, *Locusta migratoria*. Cell Tissue Res 1995;279:495–515.

[16] Dircksen H, Müller A, Keller R. Crustacean cardioactive peptide in the nervous system of the locust, *Locusta migratoria*: an immunocytochemical study on the ventral nerve cord and peripheral innervation. Cell Tissue Res 1991;263:439–57.

[17] Donly BC, Ding Q, Tobe SS, Bendena WG. Molecular cloning of the gene for the allatostatin family of neuropeptides from the cockroach *Diploptera punctata*. Proc Natl Acad Sci USA 1993;90:8807–11.
[18] Duve H, Johnsen AH, Maestro JL, Scott AG, Crook N, Winstanley D, Thorpe A. Identification, tissue localisation and physiological effect in vitro of a neuroendocrine peptide identical to a dipteran Leu-callatostatin in the codling moth *Cydia pomonella* (Tortricidae: Lepidoptera). Cell Tissue Res 1997;289:73–83.
[19] Duve H, Johnsen AH, Maestro JL, Scott AG, Jaros PP, Thorpe A. Isolation and identification of multiple neuropeptides of the allatostatin superfamily in the shore crab *Carcinus maenas*. Eur J Biochem 1997;250:727–34.
[20] Duve H, Johnsen AH, Maestro JL, Scott AG, Winstanley D, Davey M, East PD, Thorpe A. Lepidopteran peptides of the allatostatin superfamily. Peptides 1997;18:1301–9.
[21] Duve H, Johnsen AH, Scott AG, Yu CG, Yagi KJ, Tobe SS, Thorpe A. Callatostatins: neuropeptides from the blowfly *Calliphora vomitoria* with sequence homology to cockroach allatostatins. Proc Natl Acad Sci USA 1993;90:2456–60.
[22] Duve H, Thorpe A, Johnsen AH, Maestro JL, Scott AG, East PD. The dipteran Leu-callatostatins: structural and functional diversity in an insect neuroendocrine peptide family. In: Coast GM, Webster SG, editors. Recent advances in arthropod endocrinology. Cambridge: Cambridge University Press, 1998. pp. 229–47.
[23] Duve H, Wren P, Thorpe A. Innervation of the foregut of the cockroach *Leucophaea maderae* and inhibition of spontaneous contractile activity by callatostatin neuropeptides. Physiol Entomol 1995;20:33–44.
[24] Einarsson S, Josefsson B, Lagerkvist S. Determination of amino acids with 9-fluorenylmethyloxycarbonylchloroformate and RP-HPLC. J Chromatogr 1983;282:609–18.
[25] Elofsson R. 5-HT-like immunoreactivity in the central nervous system of the crayfish, *Pacifastacus leniusculus*. Cell Tissue Res 1983; 232:221–36.
[26] Gaus G, Kleinholz LH, Kegel G, Keller R. Isolation and characterization of red-pigment-concentrating hormone from six crustacean species. J Comp Physiol B 1990;160:373–9.
[27] Harris–Warrick RM, Nagy F, Nusbaum MP. Neuromodulation of stomatogastric networks by identified neurons and transmitters. In: Harris–Warrick RM, Marder E, Selverston AI, Moulins M, editors. Dynamic biological networks: the stomatogastric nervous system. Cambridge, MA: MIT Press, 1992. pp. 87–138.
[28] Hayes TK, Guan XC, Johnson V, Strey A, Tobe SS. Structure-activity studies of allatostatin 4 on the inhibition of juvenile hormone biosynthesis by corpora allata: the importance of individual side chains and stereochemistry. Peptides 1994;15:1165–71.
[29] Heinzel HG, Weimann JM, Marder E. The behavioral repertoire of the gastric mill in the crab, *Cancer pagurus*: an in situ endoscopic and electrophysiological examination. J Neurosci 1993;13:1793–803.
[30] Heinzel H-G, Hinterkeuser S, Skiebe P, Böhm H. Effect of injected allatostatin and crustacean cardioactive peptide on the stomatogastric networks in intact crayfish. Soc Neurosci Abstr 1997;23:1860.
[31] Holman GM, Cook BJ, Nachman RJ. Isolation, primary structure and synthesis of leucomyosuppressin, an insect neuropeptide that inhibits spontaneous contractions of the cockroach hindgut. Comp Biochem Physiol 1986;85C:329–33.
[32] Holman GM, Nachman RJ, Schoofs L, Hayes TK, Wright MS, De Loof A. The *Leucophaea maderae* hindgut preparation: a rapid and sensitive bioassay tool for the isolation of insect myotropins of other insect species. Insect Biochem 1991;21:107–12.
[33] Hooper SL, Marder E. Modulation of the lobster pyloric rhythm by the peptide proctolin. J Neurosci 1987;7:2097–112.
[34] Jorge–Rivera JC, Marder E. Allatostatin decreases stomatogastric neuromuscular transmission in the crab *Cancer borealis*. J Exp Biol 1997;200:2937–46.
[35] Kaufmann R, Spengler B, Lützenkirchen F. Mass spectrometric sequencing of linear peptides in a reflectron time-of-flight mass spectrometer using matrix-assisted laser desorption ionization. Rapid Commun Mass Spectrom 1993;7:902–10.
[36] Keller R. Crustacean neuropeptides: structures, functions and comparative aspects. Experientia 1992;48:439–48.
[37] Kingan TG. A competitive enzyme-linked immunosorbent assay: applications in the assay of peptides, steroids, and cyclic nucleotides. Anal Biochem 1989;183:283–9.
[38] Lange AB, Bendena WG, Tobe SS. The effect of the thirteen Dip-allatostatins on myogenic and induced contractions of the cockroach (*Diploptera punctata*) hindgut. J Insect Physiol 1995;41:581–8.
[39] Lange AB, Chan KK, Stay B. Effect of allatostatin and proctolin on antennal pulsatile organ and hindgut muscle in the cockroach, *Diploptera punctata*. Arch Insect Biochem Physiol 1993;24:79–92.
[40] Mangerich S, Keller R, Dircksen H. Immunocytochemical identification of structures containing putative red pigment-concentrating hormone in two species of decapod crustaceans. Cell Tissue Res 1986;245:377–86.
[41] Mangerich S, Keller R, Dircksen H, Rao KR, Riehm JP. Localization of pigment-dispersing hormone (PDH) and coexistence with FMRF-amide immunoreactivity in the eyestalks of two decapod crustaceans. Cell Tissue Res 1987;250:365–75.
[42] Marder E, Hooper SL, Siwicki KK. Modulatory action and distribution of the neuropeptide proctolin in the crustacean stomatogastric nervous system. J Comp Neurol 1986;243:454–67.
[43] Marder E, Jorge–Rivera JC, Kilman V, Weimann JM. Peptidergic modulation of synaptic transmission in a rhythmic motor system. Adv Organ Biol 1997;2:213–33.
[44] Mercier AJ, Lange AB, TeBrugge V, Orchard I. Evidence for proctolin-like and RFamide-like neuropeptides associated with the hindgut of the crayfish *Procambarus clarkii*. Can J Zool 1997;75:1208–25.
[45] Mercier AJ, Orchard I, TeBrugge V. FMRFamide-like immunoreactivity in the crayfish nervous system. J Exp Biol 1991;156:519–38.
[46] Mulloney B, Namba H, Agricola HJ, Hall WM. Modulation of force during locomotion: differential action of crustacean cardioactive peptide on power-stroke and return-stroke motor neurons. J Neurosci 1997;17:6872–83.
[47] Muren JE. Tachykinin-related neuropeptides in the Madeira cockroach: structures, distributions and actions. PhD Thesis. Stockholm University, Stockholm, Sweden, 1996.
[48] Muren JE, Nässel DR. Isolation of five tachykinin-related peptides from the midgut of the cockroach *Leucophaea maderae*: existence of N-terminally extended isoforms. Regul Pept 1996;65:185–96.
[49] Nusbaum MP, Marder E. A neuronal role for a crustacean red pigment concentrating hormone-like peptide: neuromodulation of the pyloric rhythm in the crab, *Cancer borealis*. J Exp Biol 1988;135:165–81.
[50] Nusbaum MP, Marder E. A modulatory proctolin-containing neuron (MPN). II. State-dependent modulation of rhythmic motor activity. J Neurosci 1989;9:1600–7.
[51] Pratt GE, Farnsworth DE, Fok KF, Siegel NR, McCormack AL, Shabanowitz J, Hunt DF, Feyereisen R. Identity of a second type of allatostatin from cockroach brains: an octadecapeptide amide with a tyrosine-rich address sequence. Proc Natl Acad Sci USA 1991;88: 2412–6.
[52] Pratt GE, Unnithan GC, Fok KF, Siegel NR, Feyereisen R. Structure-activity studies reveal two allatostatin receptor types in corpora allata of *Diploptera punctata*. J Insect Physiol 1997;43:627–34.
[53] Real D, Czternasty G. Mapping of serotonin-like immunoreactivity in the ventral nerve cord of crayfish. Brain Res 1990;521:203–12.
[54] Reichwald K, Unnithan GC, Davis NT, Agricola H, Feyereisen R. Expression of the allatostatin gene in endocrine cells of the cockroach midgut. Proc Natl Acad Sci USA 1994;91:11894–8.
[55] Rudolph PH, Stay B. Cockroach allatostatin-like immunoreactivity in the central nervous system of the freshwater snails *Bulinus globosus* (Planorbidae) and *Stagnicola elodes* (Lymnaeidae). Gen Comp Endocrinol 1997;106:241–50.

[56] Sandeman D, Sandeman R, Derby C, Schmidt M. Morphology of the brain of crayfish, crabs, and spiny lobsters: a common nomenclature for homologous structures. Biol Bull 1992;183:304–26.
[57] Sandeman DC, Sandeman RE, Aitken AR. An atlas of serotonin-containing neurons in the optic lobes and brain of the crayfish *Cherax destructor*. J Comp Neurol 1988:269.
[58] Siwicki KK, Bishop CA. Mapping of proctolinlike immunoreactivity in the nervous systems of lobster and crayfish. J Comp Neurol 1986;243:435–53.
[59] Skiebe P. Allatostatin-like immunoreactivity in the stomatogastric nervous system and the pericardial organs of the crab *Cancer pagurus*, the lobster *Homarus americanus*, and the crayfish *Cherax destructor* and *Procambarus clarkii*. J Comp Neurol 1999;403:85–105.
[60] Skiebe P, Schneider H. Allatostatin peptides in the crab stomatogastric nervous system: inhibition of the pyloric motor pattern and distribution of allatostatin-like immunoreactivity. J Exp Biol 1994; 194:195–208.
[61] Skiebe–Corrette P, Jorge–Rivera JC, Marder E. The allatostatins influence the gastric system of the crab, *Cancer borealis* (Abstract). Soc Neurosci Abstr 1993;19:931.
[62] Skowsky WR, Fisher DA. The use of thyroglobulin to induce antigenicity to small molecules. J Lab Clin Med 1972;80:134–44.
[63] Smart D, Johnston CF, Curry WJ, Williamson R, Maule AG, Skuce PJ, Shaw C, Halton DW, Buchanan KD. Peptides related to the *Diploptera punctata* allatostatins in non-arthropod invertebrates: an immunocytochemical survey. J Comp Neurol 1994;347:426–32.
[64] Smart D, Johnston CF, Maule AG, Halton DW, Hrckova G, Shaw C, Buchanan KD. Localization of *Diploptera punctata* allatostatin-like immunoreactivity in helminths: an immunocytochemical study. Parasitology 1995;110:87–96.
[65] Smith PK, Krohn RI, Heramanson GT. Measurement of protein using bicinchoninic acid. Anal Biochem 1985;150:76–85.
[66] Spengler B, Kirsch D, Kaufmann R, Jaeger E. Peptide sequencing by matrix-assisted laser-desorption mass spectrometry. Rapid Commun Mass Spectrom 1992;6:105–8.
[67] Stangier J, Hilbich C, Burdzik S, Keller R. Orcokinin: a novel myotropic peptide from the nervous system of the crayfish, *Orconectes limosus*. Peptides 1992;13:859–64.
[68] Stangier J, Keller R. Occurrence of the crustacean cardioactive peptide (CCAP) in the nervous system of the crayfish *Orconectes limosus*. In: Wiese K, Krenz WD, Tautz J, Reichert H, Mulloney B, editors. Frontiers in crustacean neurobiology. Basel: Birkhäuser, 1990. pp. 394–400.
[69] Stangier J, Keller R. Biological effects of crustacean cardioactive peptide (CCAP), a putative neurohormone/neurotransmitter from crustacean pericardial organs. In: Florey E, Stefano GB, editors. Comparative aspects of neuropeptide function. Oxford: Pergamon Press, 1992. pp. 201–10.
[70] Stay B, Chan KK, Woodhead AP. Allatostatin-immunoreactive neurons projecting to the corpora allata of adult *Diploptera punctata*. Cell Tissue Res 1992;270:15–23.
[71] Stay B, Fairbairn S, Yu CG. Role of allatostatins in the regulation of juvenile hormone synthesis. Arch Insect Biochem Physiol 1996;32: 287–97.
[72] Stay B, Tobe SS, Bendena WG. Allatostatins: identification, primary structures, functions and distribution. Adv Insect Physiol 1994;25: 267–337.
[73] Stefanini M, De Martino C, Zamboni L. Fixation of ejaculated spermatozoa for electron microscopy. Nature (London) 1967;216:173–4.
[74] Tierney AJ, Blanck J, Mercier J. FMRFamide-like peptides in the crayfish (*Procambarus clarkii*) stomatogastric nervous system: distribution and effects on the pyloric motor pattern. J Exp Biol 1997; 200:3221–33.
[75] Tobe SS, Yu CG, Bendena WG. Allatostatins, peptide inhibitors of juvenile hormone production in insects. In: Davey KG, Peter RE, Tobe SS, editors. Perspectives in comparative endocrinology. Ottawa, Ontario, Canada: National Research Council of Canada, 1994. pp. 12–9.
[76] Trube A, Audehm U, Dircksen H. Crustacean cardioactive peptide-immunoreactive neurons in the ventral nervous system of crayfish. J Comp Neurol 1994;348:80–93.
[77] Van Harreveld A. A physiological solution for freshwater crustaceans. Proc Soc Exp Biol Med 1936;34:428–32.
[78] Vanden Broeck J, Veelaert D, Bendena WG, Tobe SS, De Loof A. Molecular cloning of the precursor cDNA for schistostatins, locust allatostatin-like peptides with myoinhibiting properties. Mol Cell Endocrinol 1996;122:191–8.
[79] Veelaert D, Devreese B, Schoofs L, Van Beeumen J, Vanden Broeck J, Tobe SS, De Loof A. Isolation and characterization of eight myoinhibiting peptides from the desert locust, *Schistocerca gregaria*: new members of the cockroach allatostatin family. Mol Cell Endocrinol 1996;122:183–90.
[80] Veenstra JA, Lehman HK, Davis NT. Allatotropin is a cardioacceleratory peptide in *Manduca sexta*. J Exp Biol 1994;188:347–54.
[81] Veenstra JA, Noriega FG, Graf R, Feyereisen R. Identification of three allatostatins and their cDNA from the mosquito *Aedes aegypti*. Peptides 1997;18:937–42.
[82] Vitzthum H, Homberg U, Agricola H. Distribution of Dip-allatostatin I-like immunoreactivity in the brain of the locust *Schistocerca gregaria* with detailed analysis of immunostaining in the central complex. J Comp Neurol 1996;369:419–37.
[83] Weaver RJ, Edwards JP, Bendena WG, Tobe SS. Structures, functions and occurrences of insect allatostatic peptides. In: Coast GM, Webster SG, editors. Recent advances in arthropod endocrinology. Cambridge: Cambridge University Press, 1998. pp. 3–32.
[84] Webster SG. Amino acid sequence of putative moult-inhibiting hormone from the crab *Carcinus maenas*. Proc R Soc Lond B Biol Sci 1991;244:247–52.
[85] Weimann JM, Marder E, Evans B, Calabrese RL. The effects of SDRNFLRFamide and TNRNFLRFamide on the motor patterns of the stomatogastric ganglion of the crab *Cancer borealis*. J Exp Biol 1993;181:1–26.